Inductive heating of exhaust aftertreatment system

Kim Karlsson
Ludvig Nilsson

December 20, 2017

Acknowledgements

We would like to thank Volvo Trucks and IPROD at LTH for giving us the opportunity to perform this master thesis. In the same way we also want to say a big thanks to our handlers Tord Cedell and Kenneth Frogner, and our examiner Mats Andersson for all the support.

We would also like to direct a special thank you to Ville Akujärvi for all the help with troubleshooting, and Svante Bouvin and Mikael Hörndahl for the much needed guidance in the workshop!

This master thesis wouldn't have been possible without all of your support!

Abstract

Heavy trucks are commonly powered by combustion engines running on diesel. Since these trucks often run on highways they rarely have to perform cold starts. Diesel engines take care of their NO_x emissions through a process which uses the high temperatures of the exhaust gases together with urea, sprayed upon a mixer placed inside the exhaust pipes, to chemically react with the NO_x over an SCR catalyst. With hybrid drivetrains increasing in popularity and their inherent increased frequency of cold starts the NO_x treatment at cold starts has become a problem that needs to be solved since the reaction need to reach a critical temperature to occur. This study uses physics simulations and the building of a prototype to evaluate the possibilities of solving this problem by heating the mixer through induction heating. This report shows the possibility given a number of key changes that need to be made in order to allow for the mixer to heat the exhaust gases at cold starts.

Table of contents

1 Introduction

1.1 Background

During the combustion process in diesel powered internal combustion engines (ICE) the fuel is ignited by the high temperature caused when the fuel and air mixture is being compressed. The high temperature and high pressure are conditions which favour the the formation of NO_x[1]. In europe, heavy duty diesel engines follow emission standards known as Euro I to Euro VI. Since Euro I was introduced the allowed emission of NO_x has kept decreasing[2]. In order to meet the NO_x regulations Selective Catalytic Reduction (SCR) is used where urea is injected to the exhaust gases in the form of a water based solution called AdBlue. When the water has evaporated the urea may decompose to ammonia, the ammonia in turn react with the NO_x over the SCR catalyst ending up with Nitrogen and H_2O[3]. The SCR needs to reach temeperatures of about 200°C to work properly which is fine at operating temperature but can be a problem before the exhaust gases has reached a high enough temperature to both evaporate the water and convert the urea. With the efforts put in to decrease the impact on the environment hybrid drivetrains has increased in popularity. The hybrid drivetrains offer more efficient use of the consumed fuel as the electrical motor allows the ICE to work at as optimal operating points as is possible[4]. As the hybrid control system might shut off the ICE for a while allowing it to run at higher power at an optimal operating point when turned on, the hybrid drivetrains inherently will be more prone to cold starts. The more frequent cold starts cause the SCR to spend a larger portion of its operating time in conditions where the NO_x treatment is not working with desired performance. In order to allow the SCR to work at more efficient temperatures some heating of the exhaust gases may be needed before, or at, the mixing stage.

This master thesis is based on a prestudy made at the Division of Production and Materials Engineering at Lund University, for Volvo Group Trucks Technology. The suggested heating solution is to utilize induction to heat the mixer and mixpipe, and evaluate if the current layout of the Exhaust Aftertreatment System is feasible or how it needs to be modified in order to achieve sufficient heating.

1.2 Purpose

The purpose of this thesis is to evaluate the potential of using an inductive heating solution to heat exhaust gases at ICE cold starts. Since the SCR-

method uses an urea mixer in the mixing pipe the main part of the study has been focused on inducing heat in the mixer.
Questions this report sets out to answer are:

- Can induction heating be used to heat the exhaust gases at cold starts?
- What changes needs to be made to the system in order for it to work?
- Can the heating be done fast enough to have an effect after a few seconds?

2 Methodology

2.1 Theory

Induction heating is a non-contact method to quickly heat conductive materials by rapidly varying a magnetic field through the object that induces currents in the object material.
The magnetic field is achieved by applying an alternating current in close proximity to the object, as current paths give rise to a magnetic field according to Ampère's Law, [5].

$$\oint_C B \cdot dl = \mu_0 I_{enc}. \tag{1}$$

The current is commonly applied through a coil with a number of windings to increase the strength of the magnetic field. Each of the windings adds to the strength of the magnetic field in accordance to the superposition principle of Ampère's law, which gives the equation of the magnetic flux density of a solenoid [6],

$$B = \mu_0 \frac{N}{L} I. \tag{2}$$

This time-varying magnetic field induces current in objects of conductive material within the alternating field. These currents are known as eddy currents and is described by Faradays law of induction [7],

$$\varepsilon = -\frac{d\theta_B}{dt} \tag{3}$$

where ε is the electromotive force and θ_B is the magnetic flux.
According to Lenz's law the direction of the induced voltage, and thereby current will be such that it opposes the change of the magnetic field.

Since the magnetic field of the coil varies with the same frequency as the supplied alternating current this presents another parameter which can be controlled to regulate the induced current.
Because of different geometries of the object and the known skin effect phenomena of alternating current, which also applies to induced currents, different frequencies can change the way the heat is induced in the material. Due to the skin effect the current density, J, decreases exponentially with the distance from the surface according to [8]

$$J = J_s \cdot e^{-\delta/d}. \tag{4}$$

In this equation δ is the skin depth and is defined as the distance from the surface where the current density has decreased with e^{-1}, which is an decrease of approx. 63% of the current density for each distance δ.
An approximated skin depth, δ, can be calculated using [7]

$$\delta = \sqrt{\frac{\rho}{\pi f \mu}} \tag{5}$$

where ρ is the resistivity of the material, f is the frequency, and μ the permeability. Higher frequencies or materials with higher permeability result in a smaller skin depth. For a given induced current the current path cross section is reduced with smaller skin depth, resulting in a higher current concentration. It is these currents that result in resistive losses, together with magnetic hysteresis for ferromagnetic materials, that create the heating effect in the object. The absolute majority of the heating effect is due to the resistive losses. Resistive losses due to current can be calculated using Ohm's law [6],

$$U = R \cdot I, \quad P = U \cdot I \quad \Rightarrow \quad P = RI^2. \tag{6}$$

By using an assumption of both object material and magnetic field to be uniform and the material thickness d to be much smaller than δ, which is rarely completely true, a rough estimation of the resistive losses can be calculated using [8]

$$P_r = \frac{\pi^2 d^2 B^2 f^2}{6\rho} = [B = \mu_0 \frac{N}{L} I] = \frac{\mu_0^2 \pi^2 d^2 I^2 f^2}{6\rho} (\frac{N}{L})^2 \tag{7}$$

Since B describes an empty solenoid this equation will only give a rough estimate of how the parameters affect the induced power. The description of the empty solenoid will not be an accurate description of a solenoid wound around a magnetic material.
linebreak As mentioned before, in a ferromagnetic material a portion of the heating will also be a result of the magnetic hysteresis in addition to resistive losses. When an external magnetic field is applied to a ferromagnetic material the atomic dipoles of the material align with the polarity of the field. Once aligned some of the atomic dipoles will retain their position even after the magnetic field has been removed, the material is now magnetized.
The magnetization of the material will remain until an external magnetic field of the opposite polarization is applied to demagnetize and force the magnetization back to zero. If plotted in a BH-diagram the magnetization and demagnetization won't follow the same curve, and this is what's called the magnetic hysteresis.
By instead applying an alternating magnetic field, i.e a magnetic field caused

by an alternating current, creates a path in the BH-diagram called the magnetic hysteresis loop, as can be seen in figure 1.

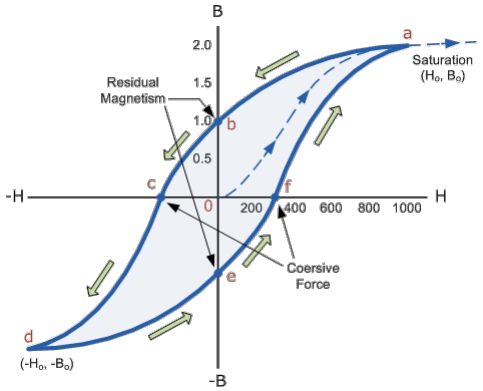

Figure 1: Source: electronics-tutorials [9]

The power loss due to hysteresis is shown as the area inside the hysteresis loop and can be calculated using [8]

$$P_m = f \cdot \int_V BH \, dV = f \cdot \int_V \mu H^2 \, dV \tag{8}$$

and the resulting total power loss of ferromagnetic materials is the sum of both resistive- and magnetic losses,

$$P_{tot} = P_r + P_m. \tag{9}$$

This results in a slightly more effective heating of ferromagnetic materials, compared to non-magnetic, but the main advantage of ferromagnetic materials is the greatly increased resistive losses due to the smaller skin depth.

2.2 Design and model building

To make necessary changes to the existing system the parts were designed in 3D using CREO Parametric. Both the mixer and mixpipe were designed in CREO and redesigned with changes made in order to observe how the heating performance was affected. The selected mixers and mixpipes were combined which created a number of geometries.

The geometries of mixers and mixpipes were imported to COMSOL Multiphysics 5.2a where the simulations were performed.

3 Mixer and mixpipe design

The models used were split up in two individual parts, the mixer and the mixpipe. The first iteration of both the mixer and mixpipe were designed to be similar to what was being used to mix the injected AdBlue. Both the mixer and mixpipe were redesigned into different versions to improve performance of the heating. The changes made on the mixer were focused on the blades while the changes on the mixpipe opened it up in order to let the magnetic field through to the mixer. Both the mixer and mixpipe were designed to be periodic with nine identical 40° slices of the whole mixer. Mixers and mixpipes from this section were combined in different combinations and used for the simulations. For all the mixpipes their outer diameter was 145.5 mm with an inner diameter of 143.5 mm. Mixers 1 to 4 had an outer diameter of 139.5 mm and inner diameter of 135.5 mm. Since Mixer 5 did not have an wall like mixers 1 to 4 the blades were attached directly to the inside of the mixpipe.

3.1 Mixer 1

Mixer 1 was a mixer design similar to existing mixers that were already being used. The hole in the middle of the existing mixers was recreated with a circular cut out of 30 mm. The modifications from the existing mixers were made to get a good geometry for the simulations and to fit the mixer in a good way into the simulated volume. Mixer 1 can be seen in figure 2.

(a) Simulation piece (b) Full mixer

Figure 2: Mixer 1

3.2 Mixer 2

Mixer 2 was based on Mixer 1 but with an attached circle, made of the same material as the mixer, in the middle. The circle in the middle was attached directly where the hole in Mixer 1 starts and the material of the circle was 2 mm thick. Since the blades of Mixer 1 were separate the idea of the attached circle in the middle was to allow for currents to flow between the blades closer to the center of the model allowing the blades to heat up further in. Mixer 2 can be seen in figure 3.

(a) Simulation piece (b) Full mixer

Figure 3: Mixer 2

3.3 Mixer 3

Mixer 3 was based on Mixer 1 but with the blades tilted upwards in a 45° angle. As in Mixer 1 the circular cut out in the middle had a 30 mm diameter. The upwards angling of the blades was intended to allow the blades to avoid the shielding of the mixer wall which would allow currents to be induced in the mixer blades. Mixer 3 can be seen in figure 4.

(a) Simulation piece (b) Full mixer

Figure 4: Mixer 3

3.4 Mixer 4

Mixer 4 was based on Mixer 3 but with an attached circle, made of the same material as the mixer, in the middle. The circle in the middle is attached directly where the hole in Mixer 3 starts and the material of the circle is 2 mm thick. The combination of mixers 2 and 3 was made to show both mixer improvements working together. Mixer 4 can be seen in figure 5.

(a) Simulation piece (b) Full mixer

Figure 5: Mixer 4

3.5 Mixer 5

Mixer 5 was designed differently from the other mixers as it did not have the mixer wall that the other mixers had. Instead of attaching the outer

mixer wall to the mixpipe, the blades were fixed directly to the mixpipe. With the outsides of the blades fixed to the mixpipe, they were held together in the middle by a cylindrical shape with rounded top and bottom. This design was made without a mixer wall in order to reduce the shielding of the magnetic field. Since the blades were attached directly to the mixpipe they would receive a better heat transfer from the mixpipe. Mixer 5 can be seen in figure 6.

(a) Simulation piece

(b) Full mixer

Figure 6: Mixer 5

3.6 Mixpipe 1

Mixpipe 1 was designed to be as similar as possible to the existing mixpipe. The inside of the mixpipe had a 1 mm gap to the outside of the mixer, and the mipxpipe was 1 mm thick. Mixpipe 1 can be seen in figure 7.

(a) Mixpipe 1 (b) Mixpipe 1 mounted with Mixer 1

Figure 7: Mixpipe 1

3.7 Mixpipe 2

Mixpipe 2 was based on Mixpipe 1 but was cut open for the lower parts of the mixer. Mixpipe 2 was connected to the mixer at the top and bottom of the cut out. This design was made to allow currents to be induced in the mixer wall. Mixpipe 2 can be seen in figure 8.

(a) Mixpipe 2 (b) Mixpipe 2 mounted with Mixer 1

Figure 8: Mixpipe 2

3.8 Mixpipe 3

Mixpipe 3 was based on Mixpipe 1 with the difference that Mixpipe 3 had a slit cut out in the wall. The slit extended over the top and bottom of the mixer it was paired with. The width of the slit was one degree, which

roughly equals to 1.27 mm. The slits of Mixpipe 3 were made to allow for the magnetic field to pass through the mixpipe and induce currents in the mixer. Mixpipe 3 can be seen in figure 9.

(a) Mixpipe 3 (b) Mixpipe 3 mounted with Mixer 1

Figure 9: Mixpipe 3

3.9 Mixpipe 4

Mixpipe 4 was based on Mixpipe 3 but had five cut out slits per section instead of the single slit that Mixpipe 3 had. As in Mixpipe 3 each slit extended over the top and bottom of the mixer it is paired with, and the width of the slit was one degree each. The increased number of slits in Mixpipe 4 were made to show how the induced current in the mixer varies with the number of slits. Mixpipe 4 can be seen in figure 10.

(a) Mixpipe 4 (b) Mixpipe 4 mounted with Mixer 3

Figure 10: Mixpipe 4

3.10 Mixpipe 5

Mixpipe 5 was redesigned and was not a pipe that enclosed the mixer the same way as the four other mixpipes. Mixpipe 5 was cut open above the mixer and slightly above the bottom of the mixer wall. The removed pipe wall was replaced with solid windings without a cooling channel. This new design of Mixpipe 5 was made to allow for the mixpipe to be used as a coil, putting the windings closer to the mixer. Mixpipe 5 without the windings modeled can be seen in figure 11.

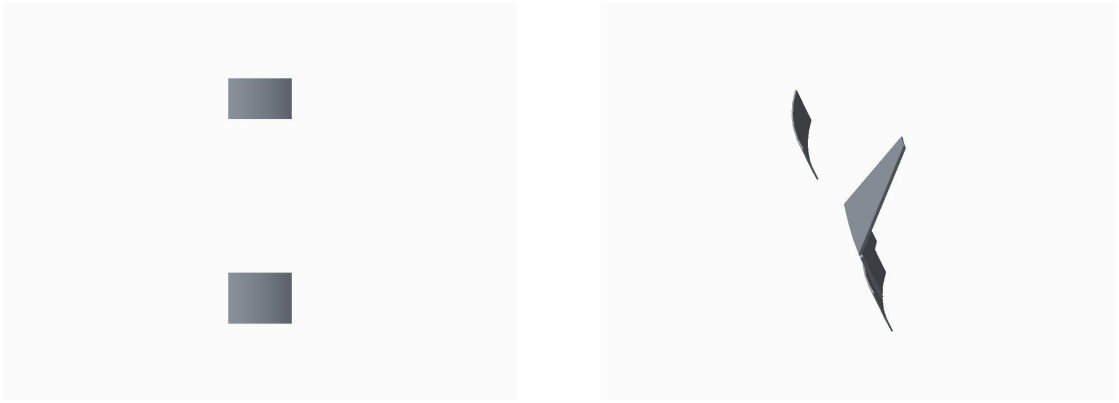

(a) Mixpipe 5 (b) Mixpipe 5 mounted with Mixer 3

Figure 11: Mixpipe 5 modeled without the windings

Since the inside of the winding was aligned with the pipe above and below the mixer, the windings were placed 1 mm from the outside of the mixer. The windings that made up the new wall were 3 mm wide and had a distance of 0.5 mm between each winding. Mixpipe 5 with the windings modeled can be seen in figure 12, here the full amount of windings are shown where they end 0.5 mm from the mixpipe on both ends. The full amount of windings caused problems with the ends of the mixpipe so the simulations were run with a few windings from the top and bottom removed.

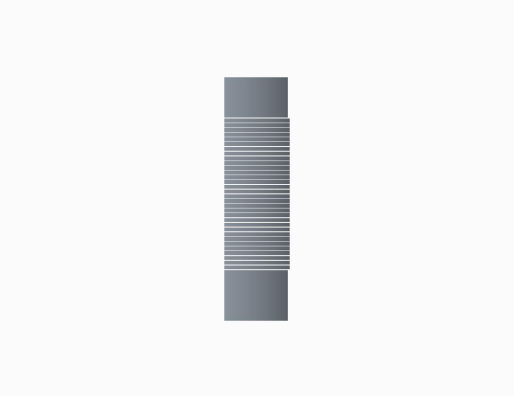

(a) Mixpipe 5

(b) Mixpipe 5 mounted with Mixer 3

Figure 12: Mixpipe 5 modelled with the windings

3.11 Mixer 1.1

Shown in figure 13 is a modified version of Mixer 1. Here the mixer wall has had some material removed in order to make a smooth corner at the bottom of the mixpipe. This variation of Mixer 1 was made to address problems occurring at the sharp corner found in mixers 1 - 4.

(a) Simulation piece

(b) Full mixer

Figure 13: Mixer 1.1

4 Simulation

4.1 Materials

The materials used in the simulation and verification were chosen with regard to their material properties to achieve the desired function, while still having a reasonable cost to make production feasible. With these parameters in mind three different materials were used.
Since the goal was to induce the heat in the mixer and not the pipe, the material used for the pipe was chosen to be AISI 316/EN 1.4404 stainless steel since this steel is non-ferritic and fulfills this requirement of minimizing induced heat generation and is the material currently used in the EATS.
Secondly, for the mixer a ferritic material was needed to maximize the induced power in the part because of the skin effect. The material chosen was AISI 430/EN 1.4016 stainless steel which is a ferritic stainless steel that is commonly used and quite cost-effective.
Lastly, the winding material was decided to be copper because of its outstanding electric conductivity ensuring minimal electrical resistance, and therefore minimize heat generation. Because of insufficient material data of the steel permeability at different temperatures and magnetic field strengths and in an effort to facilitate the calculations during simulation a few approximations of the permeability was needed. The relative permeability of the AISI 430/EN 1.4016 steel was set to a constant 2000 up to the approximate temperature of 760°C, whereas the permeability dropped to 1 over 200°C in order to implement the curie temperature. The AISI 316/EN 1.4404 stainless steel used a constant relative permeability of 1.02. Also, the relative permeability of air was set to a constant 1 to facilitate the simulations.

4.2 3D-modeling

Using Comsol Multiphysics 5.2a, physics simulation of the system was done using 3D models of the mixer and exhaust pipe with windings wound around the outside. To establish a baseline result each mixer was first simulated without a pipe wall, and then run again using each of the different pipe designs. In order to reduce computational requirements each model was partitioned into nine symmetrical slices, each a 40° slice from the center axis and was then used to simulate upon. Side edges were given a continuity periodic boundary condition to allow the heat of the material and the magnetic field to spread from one edge of the partition to another to ensure symmetry with a complete model. The air domain around the model was set to a sphere with a radii of 400 mm, with an additional 100 mm modeled as an infinite

element domain.

The number of windings was decided in such a way that they would cover the entire height of the mixer with some overshoot. This resulted in Mixer 1 and 2 having 13 windings, and Mixer 3 and 4 having 21 windings because of their increased height. Mixer 3 without a mixpipe was also simulated using 13 windings in order to be able to accurately evaluate the efficiency of the design compared to Mixer 1 and 2. Mixpipe 5 was originally meant to have windings covering the entire air gap of the pipe wall but early testing showed that too much power would be induced in the wall endings, which resulted in one winding being removed from the top and bottom for Mixers 1 & 2 and two windings removed from both top and bottom for Mixers 3 & 4. The end results for Mixpipe 5 were that Mixers 1 & 2 used 15 windings, and Mixers 3 & 4 used 28 windings. Also as a way to reduce computational resources the windings were simulated as edge currents, i.e. all current flowing through point lines around the model. By using this method the windings of the coil did not have to be meshed and simulated with skin effect, current density, temperature, etc. The edge currents were placed approximately 3.1 mm from the outer edge of the pipe, which was considered an appropriate distance for insulation between windings and mixpipe.
Depending on the skin depth at a frequency of 22 kHz different parts of different materials were modeled either with a linearized resistivity when the skin depth was of the same magnitude as the material thickness, and as a impedance boundary condition when the skin depth was much smaller than the thickness of the material.

Since implementing a CFD, computational fluid dynamics, calculation would have been far to computationally demanding and taken too much time, the heat dissipation inside the mix pipe was derived using rough estimations and applied as heat transfer coefficients to the various parts.
The coefficient used was supplied by Volvo and was given for three different airflows, but due to time constraints only the medium airflow coefficients were used in simulations. The full list of coefficients can be seen in table 1.

Airflow	Mixer wing $(W/(m^2 \cdot K))$	Pipe wall $(W/(m^2 \cdot K))$
Low Airflow	$76.1 + 0.221 \cdot (T - 293)^{0.79}$	$12.7 + 0.042 \cdot (T - 293)^{0.72}$
Medium Airflow	$162.6 + 0.571 \cdot (T - 293)^{0.76}$	$30.8 + 0.069 \cdot (T - 293)^{0.78}$
High Airflow	$345.4 + 1.995 \cdot (T - 293)^{0.69}$	$74.1 + 0.162 \cdot (T - 293)^{0.78}$

Table 1

5 Results

In this section the results of the simulations are presented. The results presented are of all combinations of Mixer 1 and, based on those results, continued with the most promising combinations of mixers and mixpipes. Since the simulations were run up to 180 seconds all of the simulated time steps will not be presented here. The time steps presented are 4 seconds for all models and 20 seconds or 120 seconds for models where the heating profile has changed significantly from the 4 second figure. Along with the figures a graph is also presented where the temperature of the measuring points in the model is shown as a function of time. The distribution of the points in the various mixers can be seen in figure 14. The distribution in Mixer 1 and Mixer 2 are the same because of their similarity, and the same applies to Mixer 3 and Mixer 4. A second graph showing the induced power in the mixer and mixpipe is also included in every section.

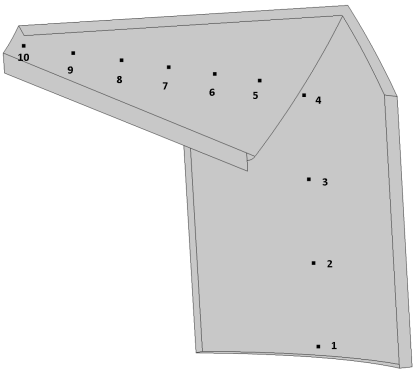

(a) Measuring point placement in Mixer 1 and 2.

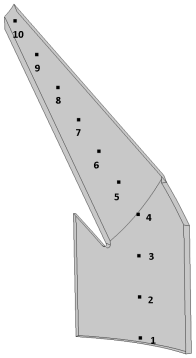

(b) Measuring point placement in Mixer 3 and 4.

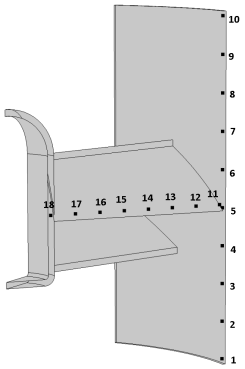

(c) Measuring point placement in Mixer 5

Figure 14: Measuring point placements in the mixers.

The figures for 4, 20 and 120 seconds, along with both graphs, for all model configurations are placed uncommented in Appendix A.

5.1 Mixer 1

Shown below is the simulation of Mixer 1 run without a mixpipe. In figure 15 the mixer temperature after 4 seconds is shown, in figure 16 are the temperatures from the measuring points in the mixer and in figure 17 is a graph over the induced power in the mixer.

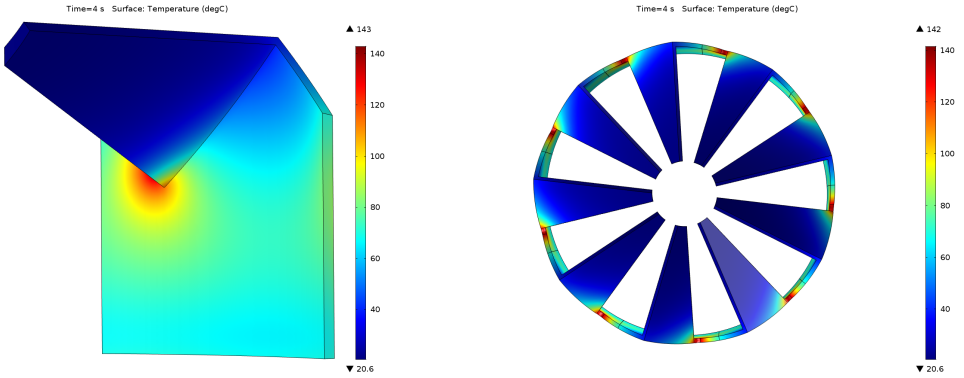

(a) 40° slice of the mixer (b) The full mixer, seen from above

Figure 15: Heating profile after 4 seconds of heating.

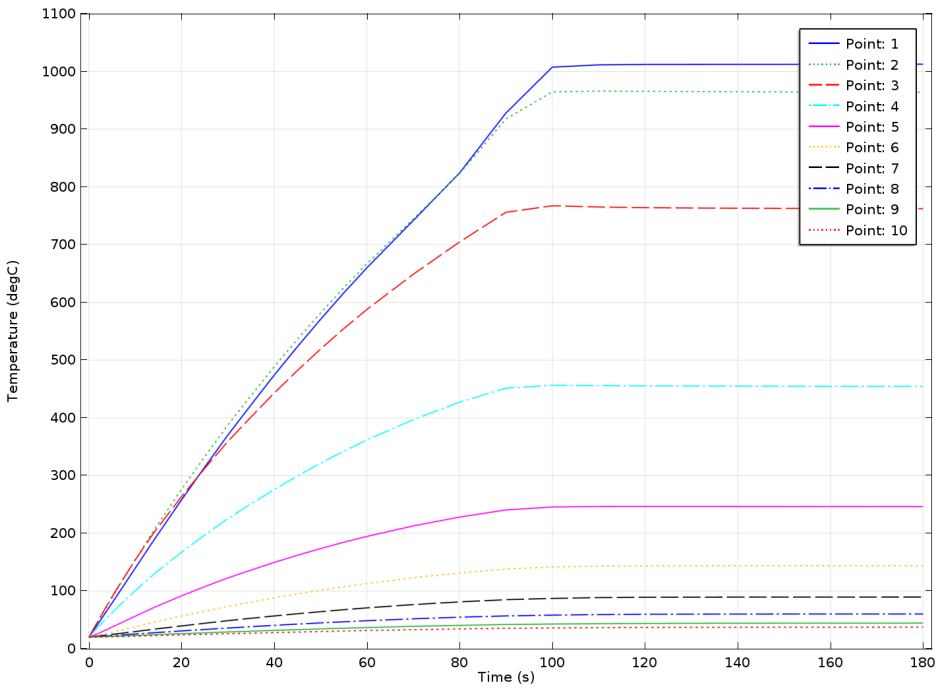

Figure 16: Graph of temperature over time in the measuring points.

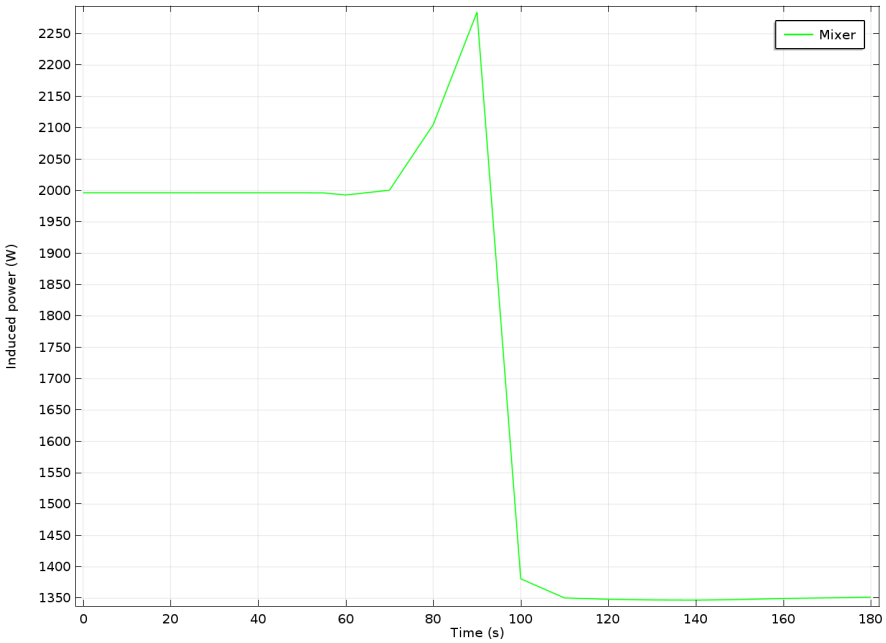

Figure 17: Graph of the induced power in the mixer.

In figure 15 it can be seen that the mixer reached a maximum temperature of 143°C and that the mixer received a strong local heating at the sharp bottom corner where the mixer blade was attached to the mixer wall. As can be seen in figure 16 the two warmest measuring points were point 1 and point 2 where measuring point 1 reached over 1000°C. The induced power in the mixer was stable at 2000 W until 70 seconds where it started increasing until it peaked at 90 seconds and over 2250 W. After 90 seconds the induced power started to decrease and at 100 seconds the induced power was less than 1400 W.

5.1.1 Mixpipe 1

The result of the simulation of Mixer 1 with Mixpipe 1 is shown below. In figure 18 the temperature after 4 seconds is shown and in figure 19 are the temperatures from the measuring points in the mixer. In figure 20 the induced power in the mixer and mixpipe is shown.

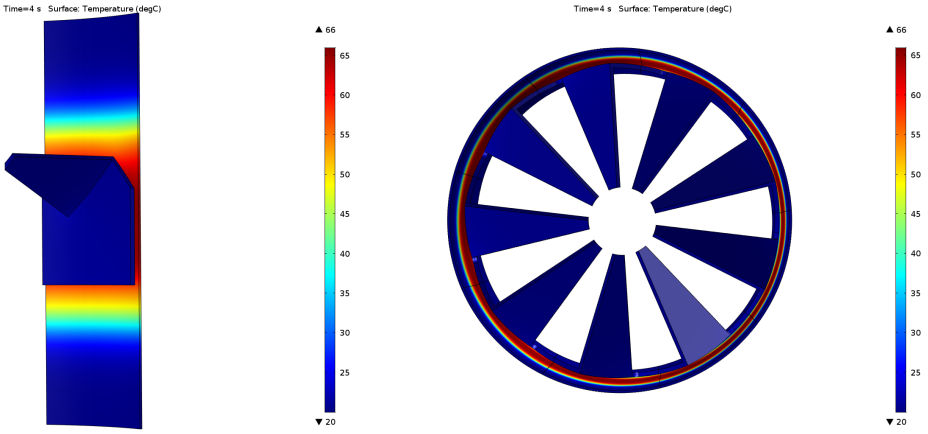

(a) 40° slice of the mixer (b) The full mixer, seen from above

Figure 18: Heating profile after 4 seconds of heating.

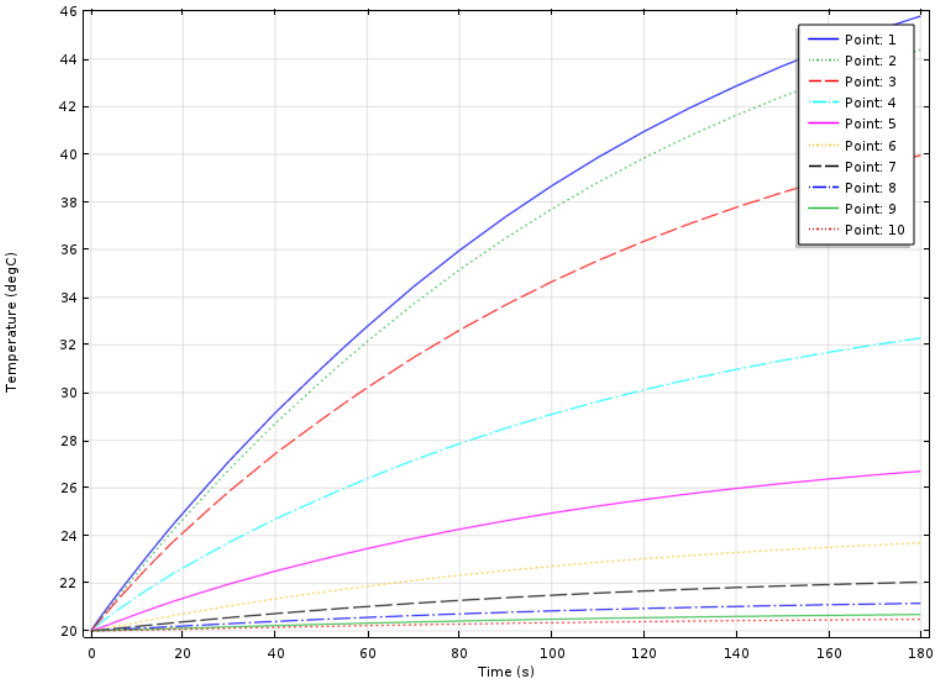

Figure 19: Graph of temperature over time in the measuring points.

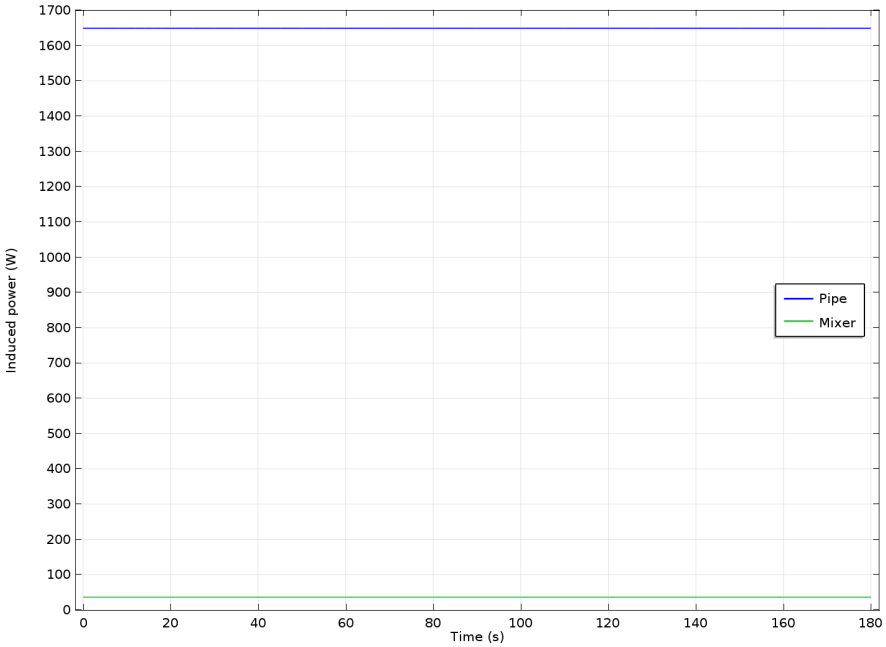

Figure 20: Graph of the induced power in both mixer and mixpipe.

As can be seen in figure 18 the maximum temperature of this model was 66°C. The heating profile of the mixpipe was an even heating distribution all around the mixpipe. The temperature of the entire mixer stayed below 30°C at 4 seconds. In figure 19 it can be seen that the temperature kept increasing for all measured points. Point 1 reached the highest temperature of the measuring points in the mixer at almost 46°C after 180 seconds. Also, in figure 20 can be seen that the absolute majority of power is induced in the mixpipe wall with only a fraction being induced in the mixer. From figure 20 it can be seen that the induced power in the mixer was less than 50 W while the induced power in the mixpipe was around 1650 W for the entire simulation.

5.1.2 Mixpipe 2

The result of the simulation of Mixer 1 with Mixpipe 2 is shown below. Figure 21 shows the temperature after 4 seconds, figure 22 are the temperature measuring points in the mixer, and figure 23 shows the induced power in the mixer and mixpipe.

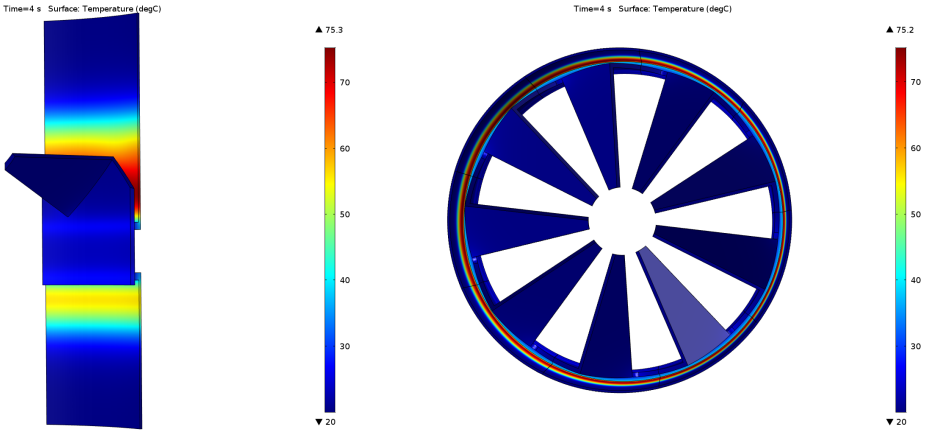

(a) 40° slice of the mixer (b) The full mixer, seen from above

Figure 21: Heating profile after 4 seconds of heating.

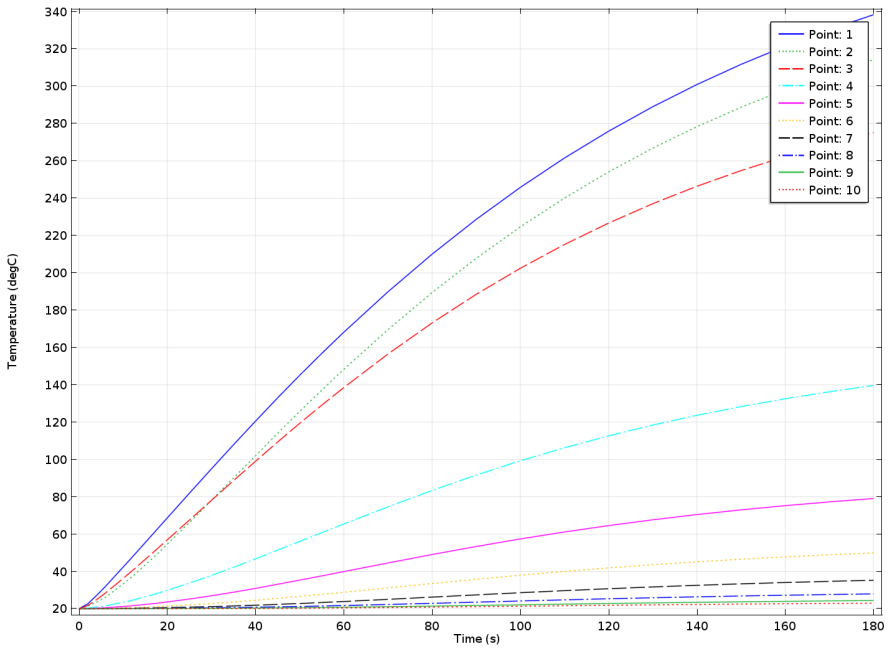

Figure 22: Graph of temperature over time in the measuring points.

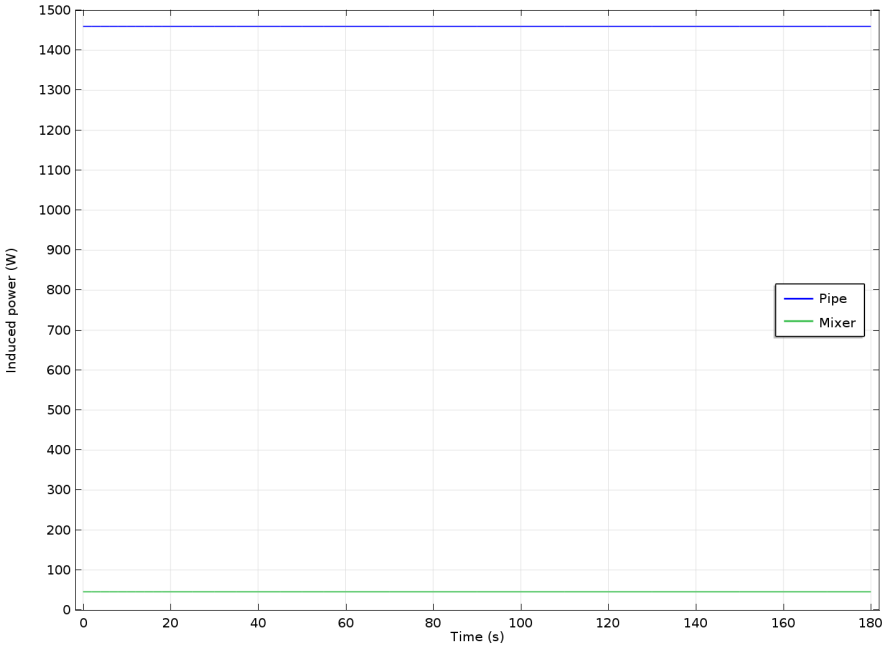

Figure 23: Graph of the induced power in both mixer and mixpipe.

As can be seen in figure 21 the highest temperature reached in this model was 75°C. The mixpipe received an even heating around the pipe with the upper part of the wall reaching higher temperatures than the lower. The wall part of the mixer increased in temperature with the parts connected to the mixpipe increasing the most. In figure 23 it can be seen that about 1650 W is induced in the mixpipe while the mixer receives less with 46 W.

5.1.3 Mixpipe 3

The result of the simulation of Mixer 1 with Mixpipe 3 is shown below. Figure 24 shows the temperature after 4 seconds, figure 25 the temperature after 120 seconds and in figure 26 are the temperature measuring points in the mixer. The induced power in the mixer and mixpipe is shown in figure 27.

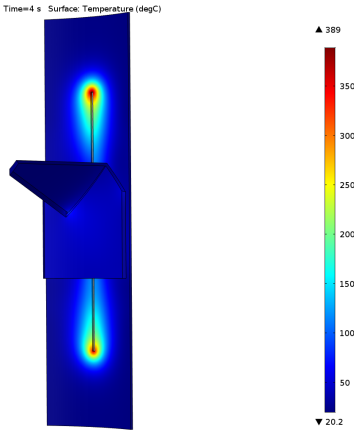

(a) 40° slice of the mixer

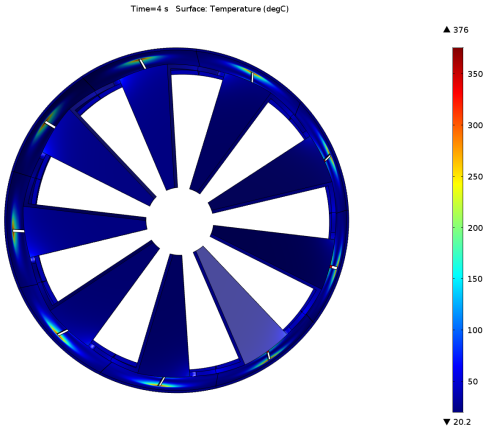

(b) The full mixer, seen from above

Figure 24: Heating profile after 4 seconds of heating.

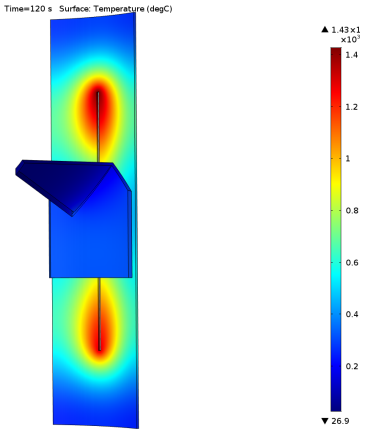

(a) 40° slice of the mixer

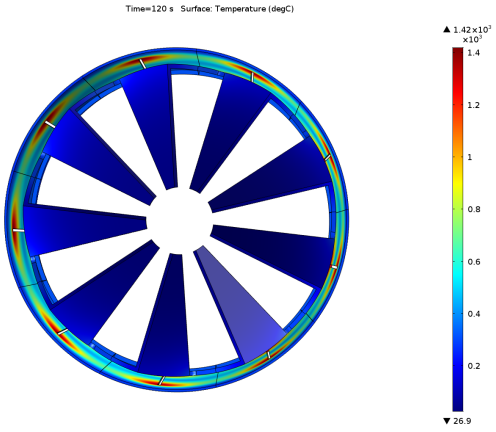

(b) The full mixer, seen from above

Figure 25: Heating profile after 120 seconds of heating.

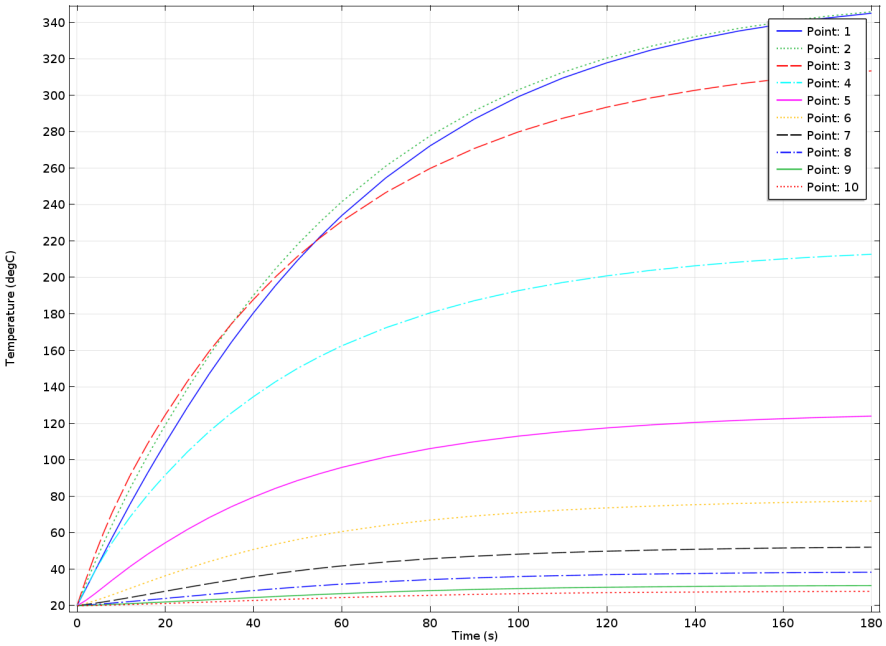

Figure 26: Graph of temperature over time in the measuring points.

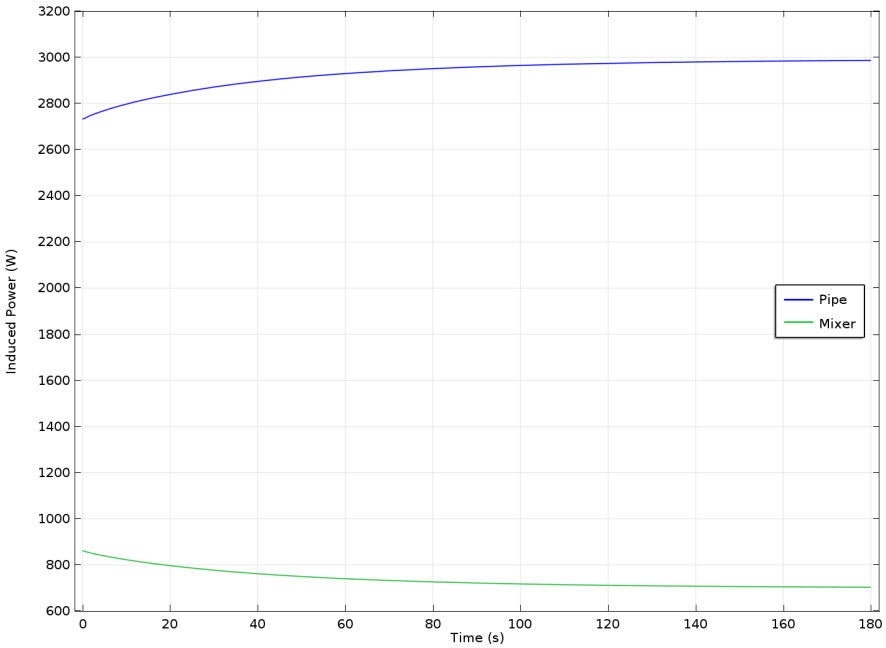

Figure 27: Graph of the induced power in both mixer and mixpipe.

In figure 24 the heating profile after 4 seconds of this model can be seen. In

this model the heating of the mixpipe was concentrated around the corners of the slits. The wall of the mixer had increased in temperature with the largest increase found at the bottom of where the blade was attached to the wall of the mixer. In figure 25a the heating profile after 120 seconds can be seen. The maximum temperature found after 120 seconds was 1430°C and was found at the corners of the mixpipe slits. Figure 26 shows the temperature of the measuring points in the mixer. Points 1, 2 and 3 increased the most in temperature with point 1 and 2 that reached over 340°C after 180 seconds. These three points were all found in the wall of the mixer. As can be seen in figure 27 the induced power in the mixpipe increased during the simulation but plateaued at slightly less than 3000 W. The induced power in the mixer decreased during the simulation and ended up at around 700 W.

5.1.4 Mixpipe 4

The result of the simulation using Mixer 1 with Mixpipe 4 is shown below. Figure 28 shows the temperature after 4 seconds, in figure 29 is the graph over the temperature measured in the measuring points of the mixer, and in figure 30 the induced power in the mixer and mixpipe is shown.

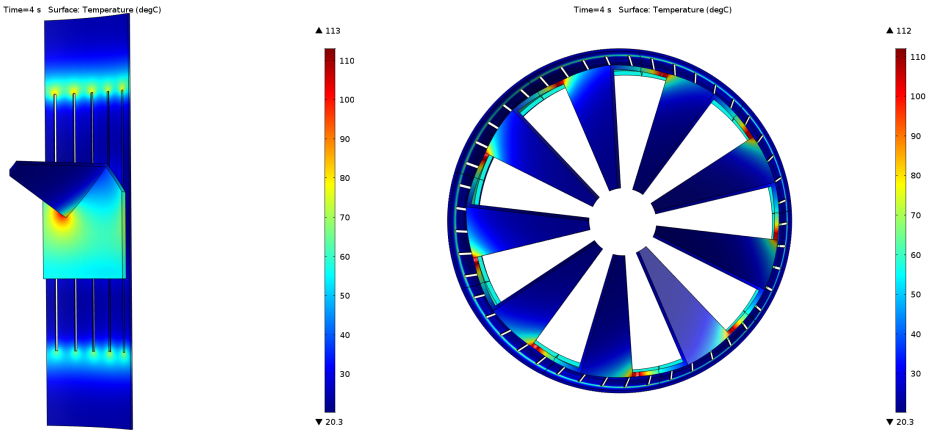

(a) 40° slice of the mixer (b) The full mixer, seen from above

Figure 28: Heating profile after 4 seconds of heating.

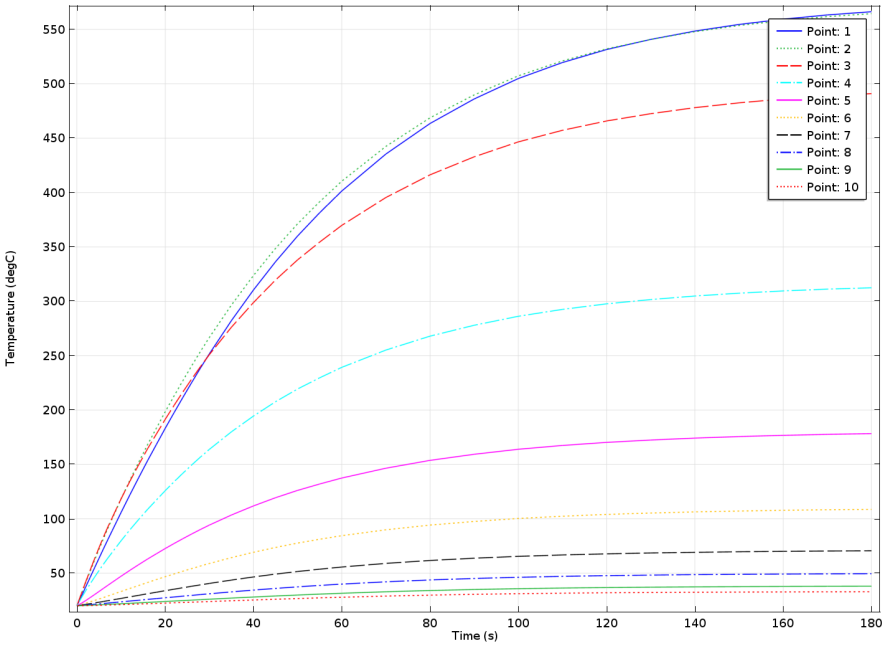

Figure 29: Graph of temperature over time in the measuring points.

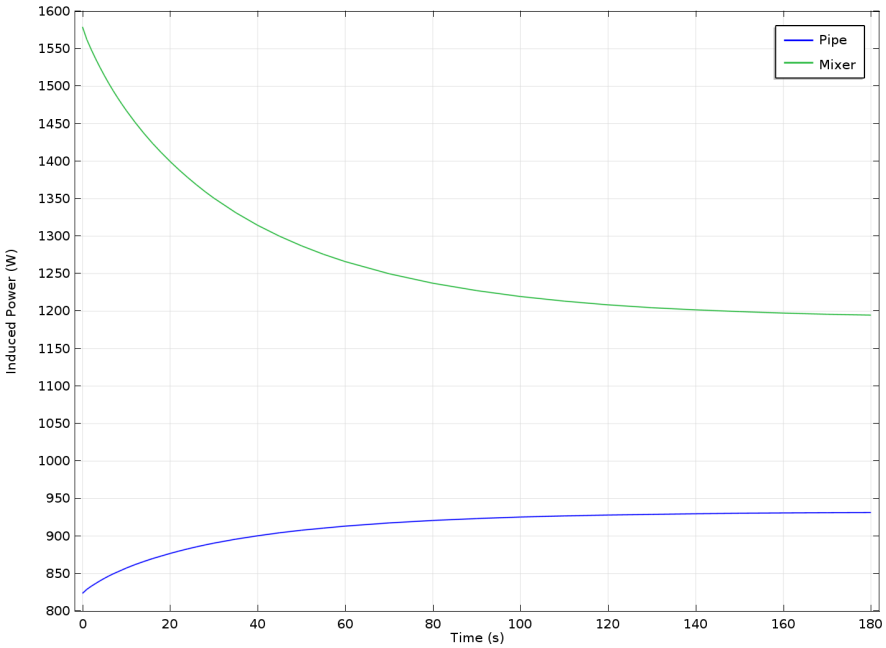

Figure 30: Graph of the induced power in both mixer and mixpipe.

In figure 28 the heating of this model after 4 seconds can be seen. The

heating of the mixpipe formed two belts around the mixer located at each end of the mixpipe slits. As seen in figure 28a the mixer received a strong local heating around the sharp bottom corner where the mixer blade is attached to the mixer wall. In figure 29 it can be seen that the measuring points in the wall were heated the most. Measuring points 1 and 2 both reached over 550°C. Looking at figure 30 it can be noted that almost 1600 W initially was induced in the mixer. The induced power of the mixer decreased during the simulation and at 180 seconds the power induced in the mixer was 1200 W. The induced power in the mixpipe increased from around 825 W to over 925 W during the simulation.

5.1.5 Mixpipe 5

The result of the simulation using Mixer 1 with Mixpipe 5 is shown below. Figure 31 shows the temperature after 4 seconds and in figure 32 is the graph over the temperature measured in the measuring points of the mixer. Shown in figure 33 is the induced power in the mixer and mixpipe.

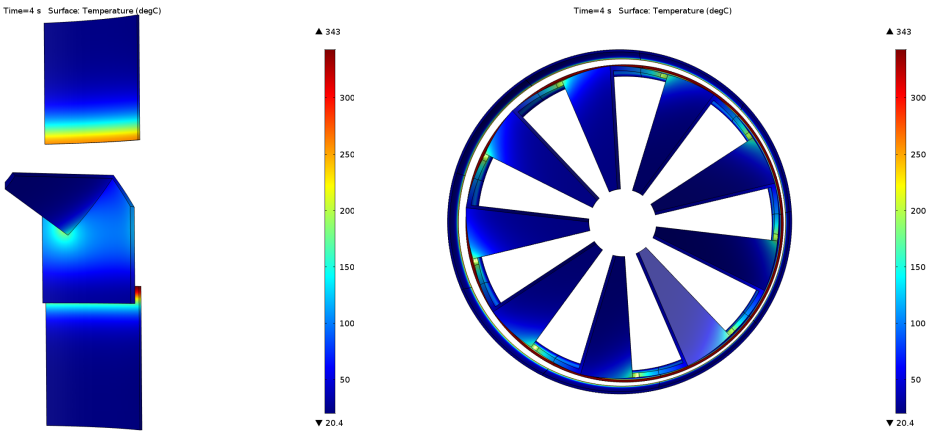

(a) 40° slice of the mixer (b) The full mixer, seen from above

Figure 31: Heating profile after 4 seconds of heating.

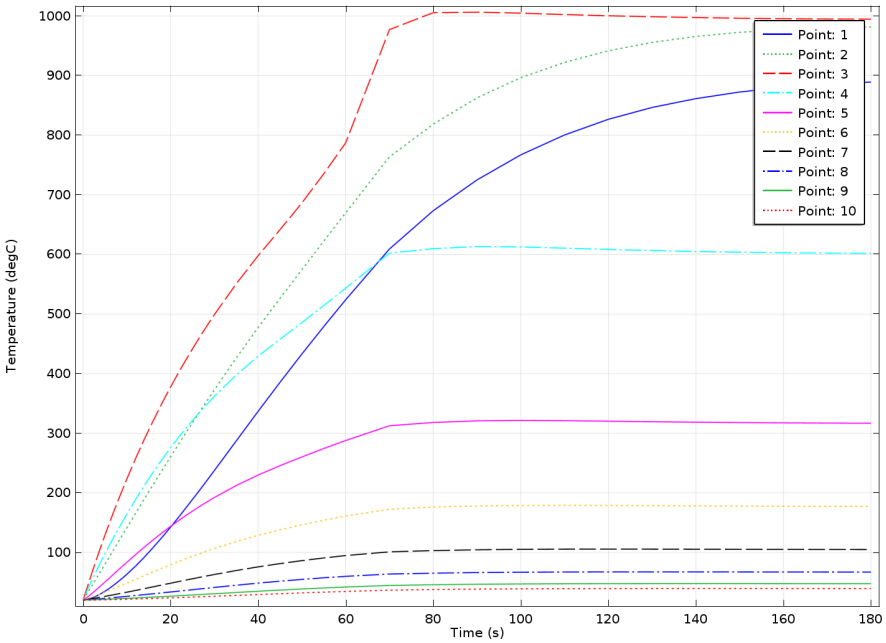

Figure 32: Graph of temperature over time in the measuring points.

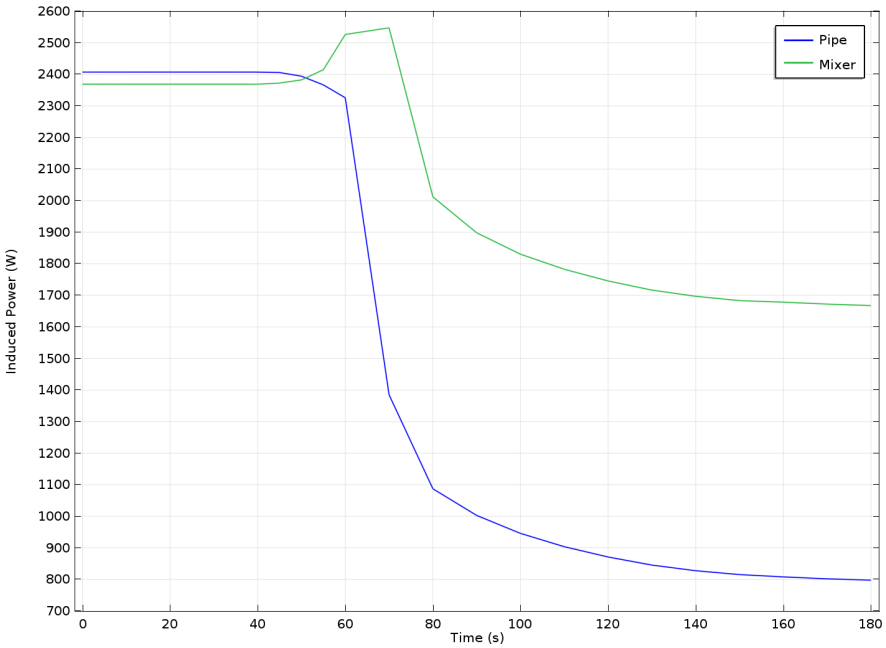

Figure 33: Graph of the induced power in both mixer and mixpipe.

In figure 31a it can be seen that the largest temperature increase of the

wall was found at the edges close to the windings of the model. It can also be seen that the mixer received a strong local heating around the sharp bottom corner where the mixer blade meets the mixer wall. As can be seen in figure 32 points 2, 3 and 4 received the most heating of all the points at the beginning of the simulation. Measuring points 1 and 2 were heated the most and both reached around 1000°C after 180 seconds. Looking at figure 33 it can be seen that the power induced in the mixpipe was at 2400 W initially but started decreasing after about 50 seconds. The power induced in the mixer started out slightly less than of the mixpipe and had a peak at roughly 70 seconds where it then started decreasing.

5.2 Mixer 2

Shown below is the simulation of Mixer 2 run without a mixpipe. Figure 34 shows the mixer temperature after 4 seconds, in figure 35 are the temperatures from the measuring points in the mixer, and in figure 36 is a graph of the induced power in the mixer.

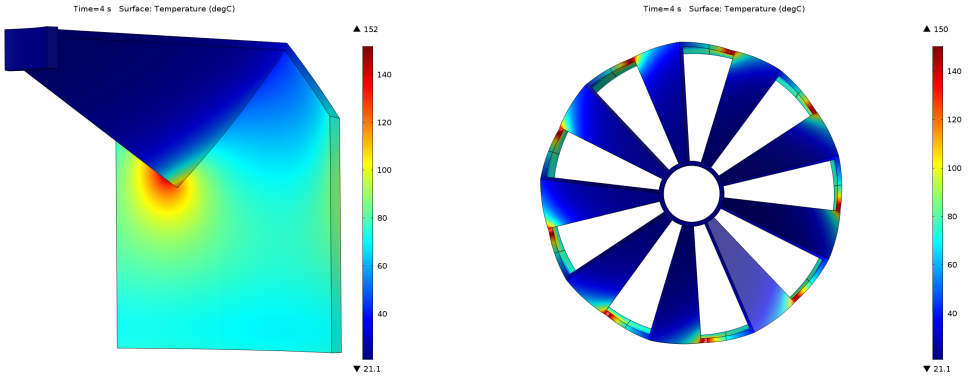

(a) 40° slice of the mixer (b) The full mixer, seen from above

Figure 34: Heating profile after 4 seconds of heating.

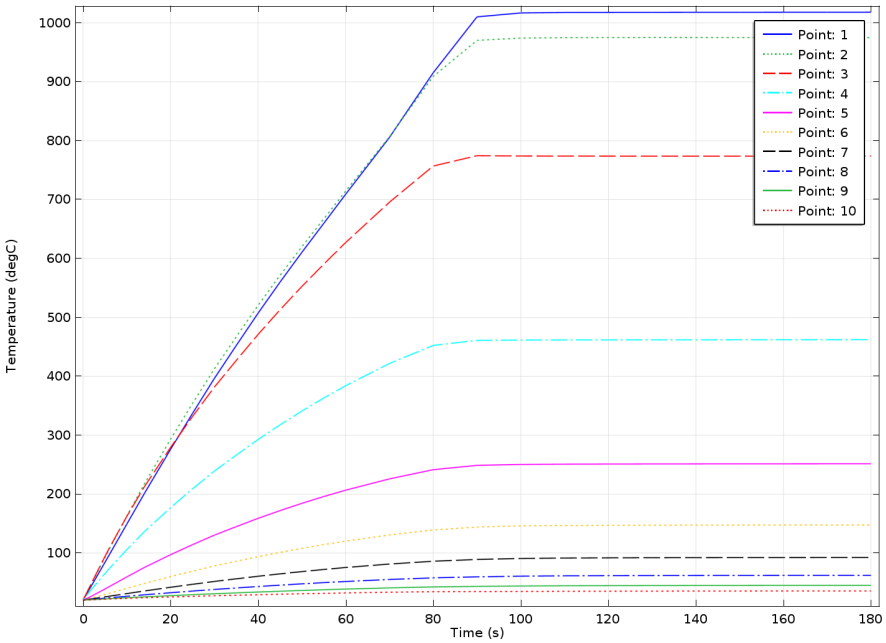

Figure 35: Graph of temperature over time in the measuring points.

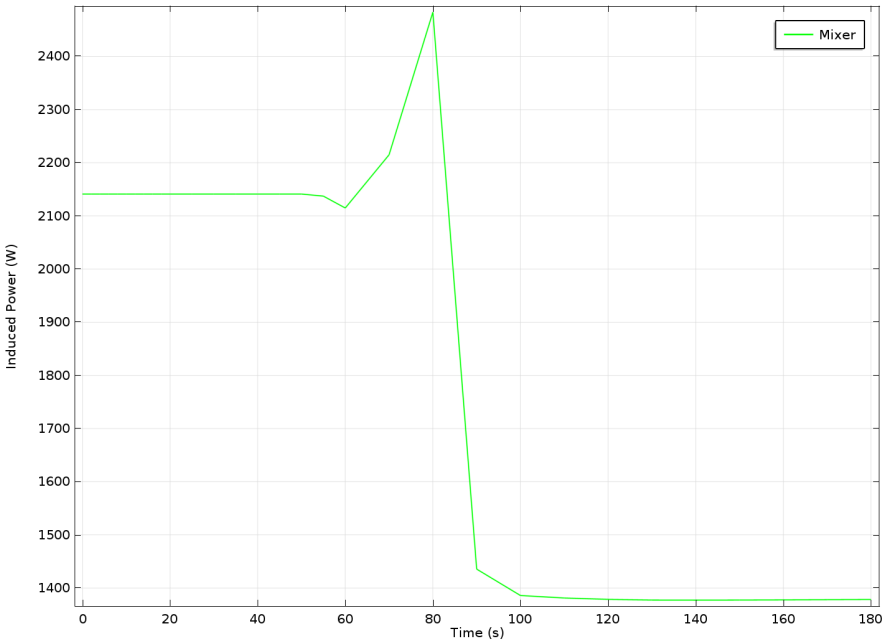

Figure 36: Graph of the induced power in the mixer.

From figure 34 it can be seen that the highest temperature of the mixer

was 152°C after 4 seconds and that the sharp corner at the bottom of the mixer blade had a strong local heating. Figure 35 shows that measuring points 1 and 2 increased the most in temperature and that measuring point 1 reached over 1000°C. The induced power in the mixer was initially around 2150 W but had a local minimum at 60 seconds to increase to a peak at 80 seconds and almost 2500 W. At 100 seconds the induced power in the mixer stabilized at slightly less than 1400 W.

5.2.1 Mixpipe 4

The result of the simulation using Mixer 2 with Mixpipe 4 is shown below. Figure 37 shows the temperature after 4 seconds, and in figure 38 is the graph over the temperature measured in the measuring points of the mixer. Shown in figure 39 is the induced power in the mixer and mixpipe.

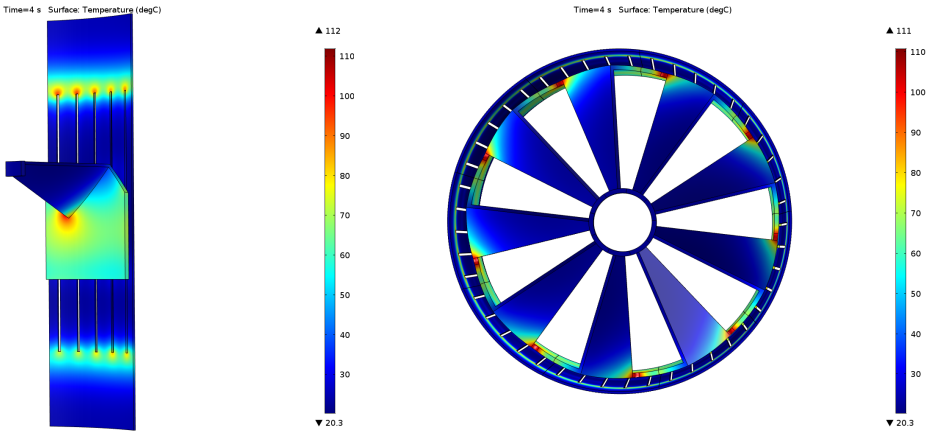

(a) 40° slice of the mixer (b) The full mixer, seen from above

Figure 37: Heating profile after 4 seconds of heating.

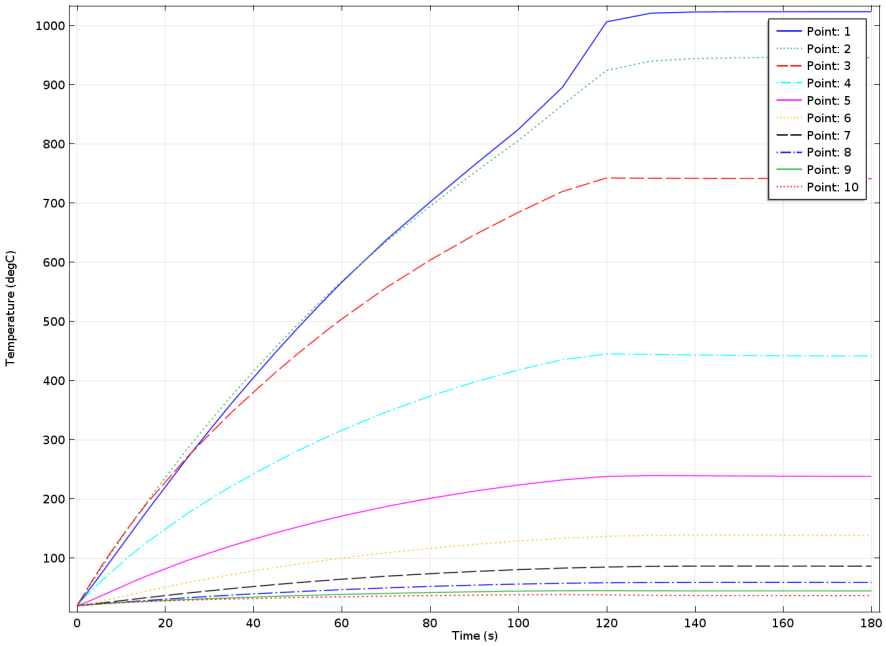

Figure 38: Graph of temperature over time in the measuring points.

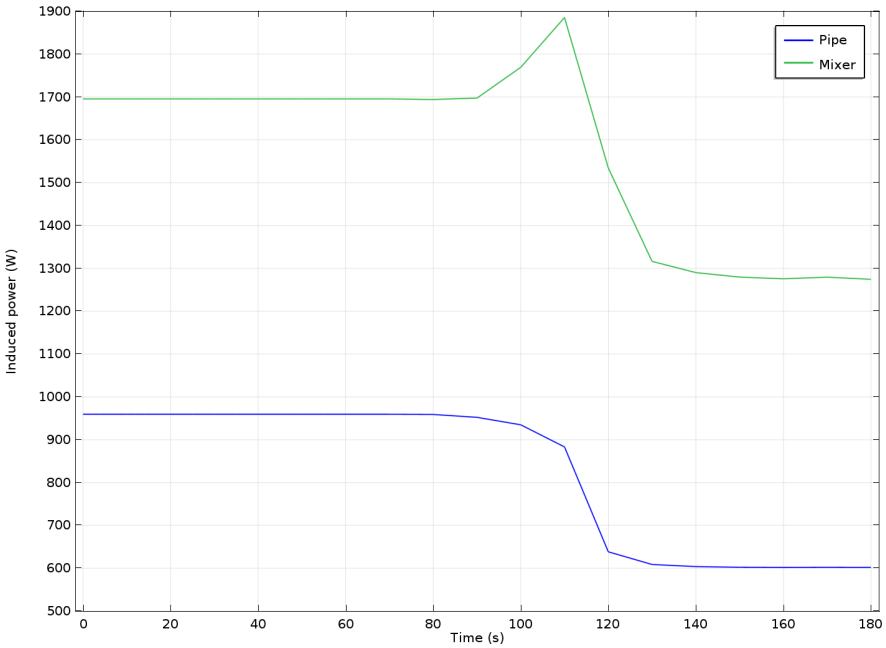

Figure 39: Graph of the induced power in both mixer and mixpipe.

As can be seen in figure 37 the mixpipe heating was concentrated around

the slits, which formed two belts around the mixpipe. The mixer was heated at most parts of the mixer wall with a strong local heating at the sharp bottom corner where the mixer blade was attached to the mixer wall. Figure 37b shows that after 4 seconds the inner parts of the mixer blades had not reveiced any large amounts of heating. As can be seen in figure 38 measuring point 3 was the warmest point for the first 15 seconds but after 120 seconds measuring point 1 reached the highest temperature at over 1000°C. The induced power of the mixer started at about 1700 W and peaked at almost 1900 W after 100 seconds which can be seen in figure 39. The mixpipe was induced with around 950 W initially. The induced power in the mixpipe was decreased from 950 W to about 600W between 80 and 140 seconds.

5.2.2 Mixpipe 5

The result of the simulation using Mixer 2 with Mixpipe 5 is shown below. Figure 40 shows the temperature after 4 seconds, in figure 41 is the graph over the temperature measured in the measuring points of the mixer and in figure 42 the induced power in the mixer and mixpipe is shown.

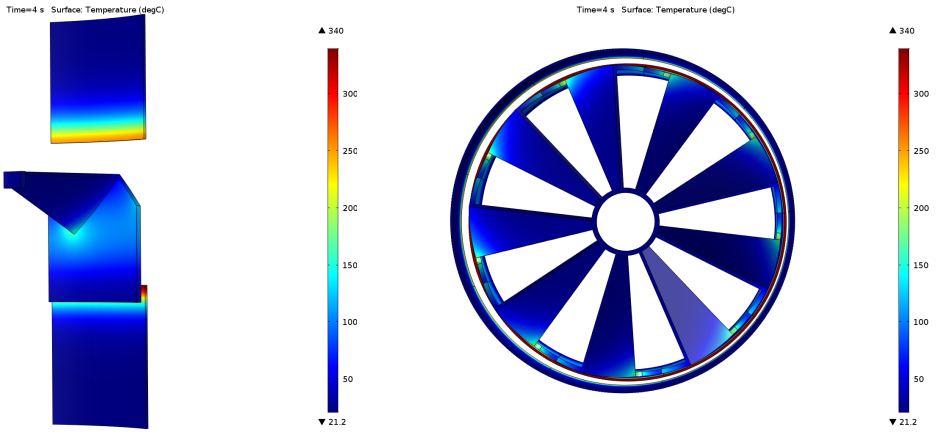

(a) 40° slice of the mixer (b) The full mixer, seen from above

Figure 40: Heating profile after 4 seconds of heating.

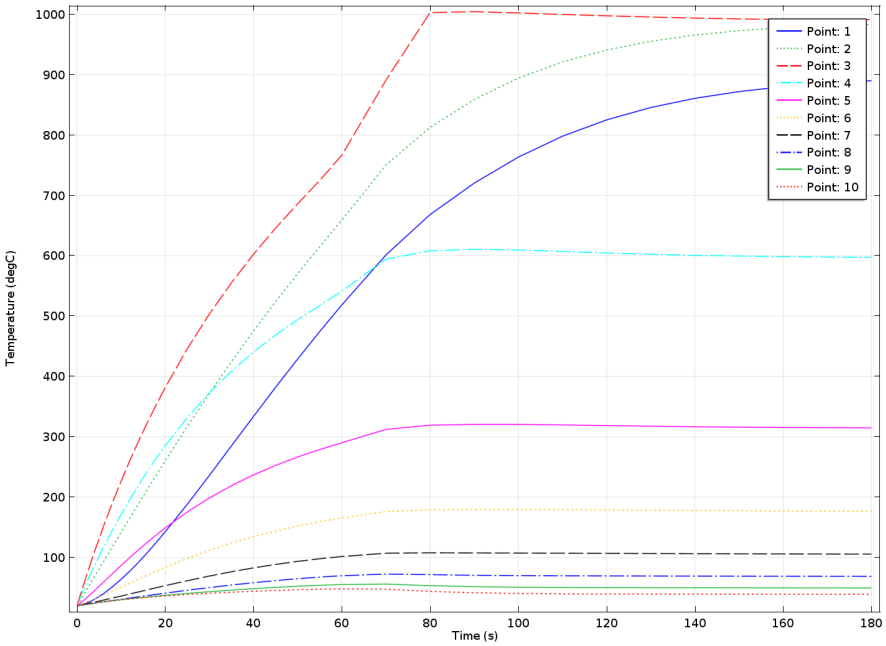

Figure 41: Graph of temperature over time in the measuring points.

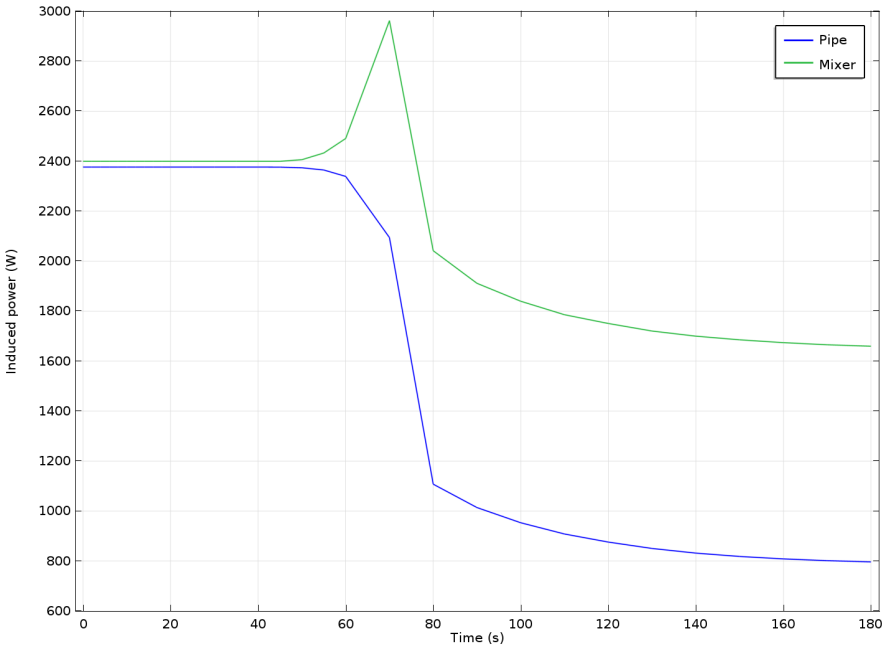

Figure 42: Graph of the induced power in both mixer and mixpipe.

In figure 40a it can be seen that the edges of the cut out wall increased

the most in temperature. The heating of the mixer was largely located to the wall where it can be seen that the top half of the mixer wall after 4 seconds was warmer than the bottom part of the mixer wall. As can be seen in figure 40b the inner parts of the mixer blades did not receive a large temperature increase. Figure 41 shows that measuring point 3 received the fastest heating of the measuring points and that it after 80 seconds had reached 1000°C where it plateaued. As can be seen in figure 42 the induced power in the mixer and mixpipe was close to each other until 50 seconds. At 50 seconds the induced power in the mixpipe started decreasing while the induced power in the mixpipe started increasing with a peak at 70 seconds.

5.3 Mixer 3

Shown below is the simulation of Mixer 3 run without a mixpipe. Figure 43 shows the mixer temperature after 4 seconds, in figure 44 are the temperatures from the measuring points in the mixer, and in figure 45 is a graph of the induced power in the mixer.

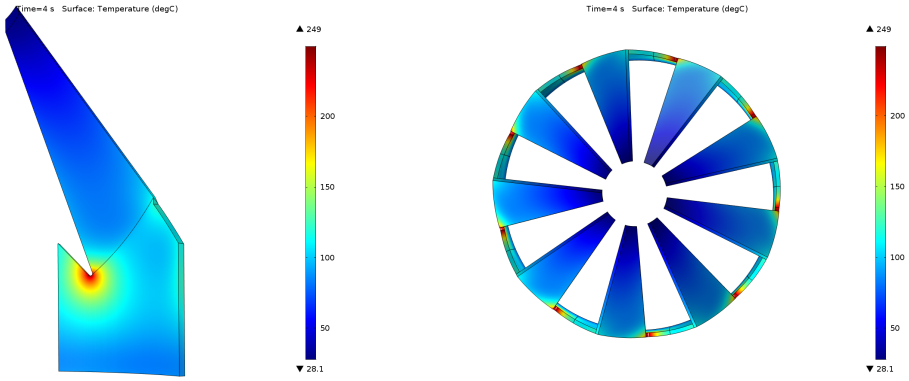

(a) 40° slice of the mixer

(b) The full mixer, seen from above

Figure 43: Heating profile after 4 seconds of heating.

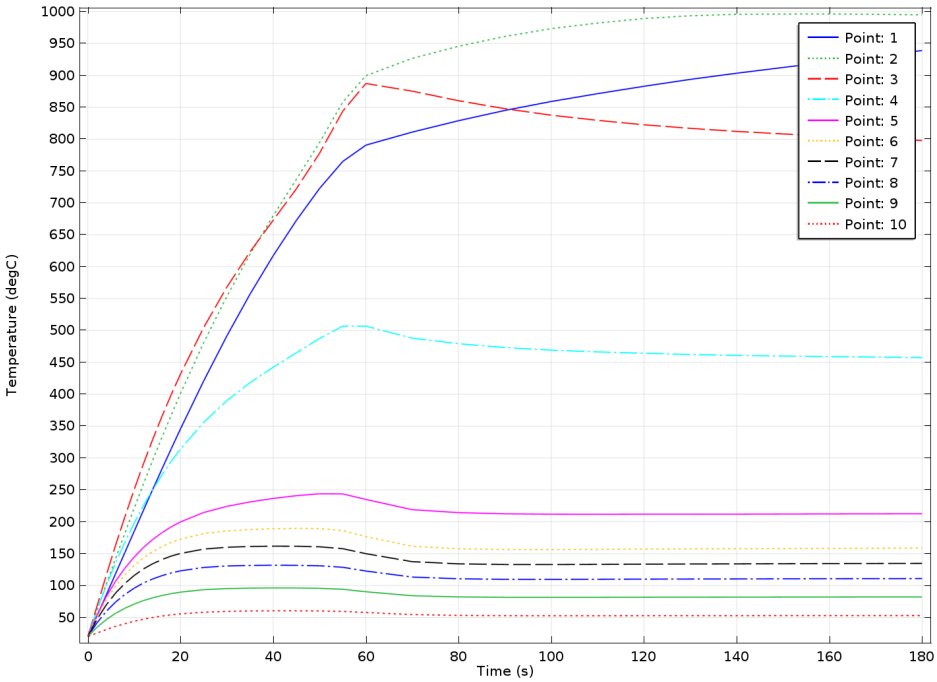

Figure 44: Graph of temperature over time in the measuring points.

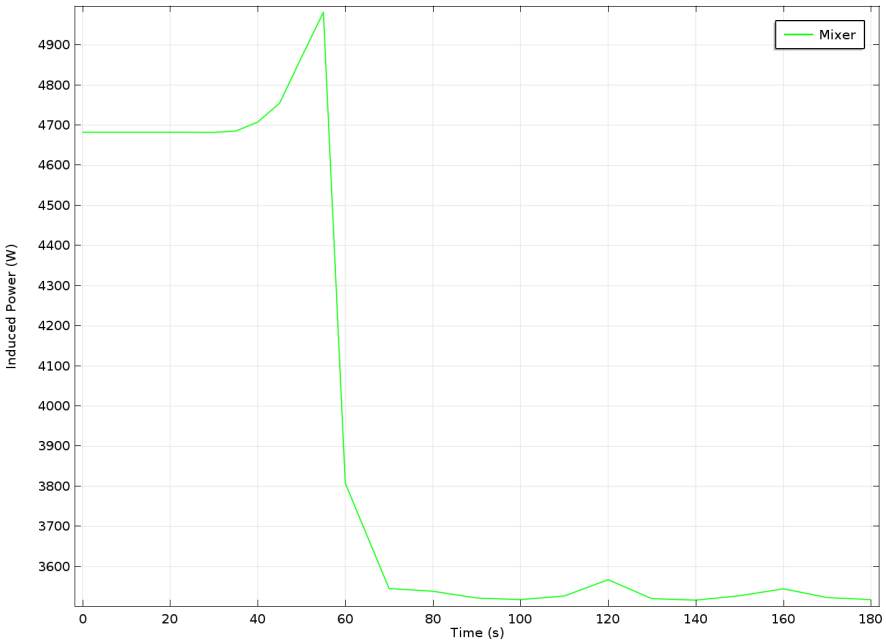

Figure 45: Graph of the induced power in the mixer.

As can be seen in figure 43 after 4 seconds the lower part of the mixer blades had reached 100°C. The sharp corner at the bottom of where the mixer blade were attached to the mixer wall had a strong heating and the highest temperature of the mixer was 249°C. From figure 44 it can be seen that measuring points 1, 2 and 3 had the highest temperatures with measuring point 2 at around 1000°C. Figure 45 shows that the induced power in the mixer initially was around 4700 W. The induced power in the mixer had a peak at 55 seconds where it had reached almost 5000 W. After the peak in power the induced power in the mixer decreased, between 70 seconds and 180 seconds the induced power in the mixer varied between 3500 W and 3600 W.

5.3.1 Mixer 3 with fewer windings

Shown below is the results of Mixer 3 simulated using the same number of windings as Mixer 1 and 2 and without a mixpipe. Figure 46 shown the temperature after 4 seconds, in figure 47 is the graph over the temperature measured in the measuring points of the mixer, and in figure 48 the induced power in the mixer is shown.

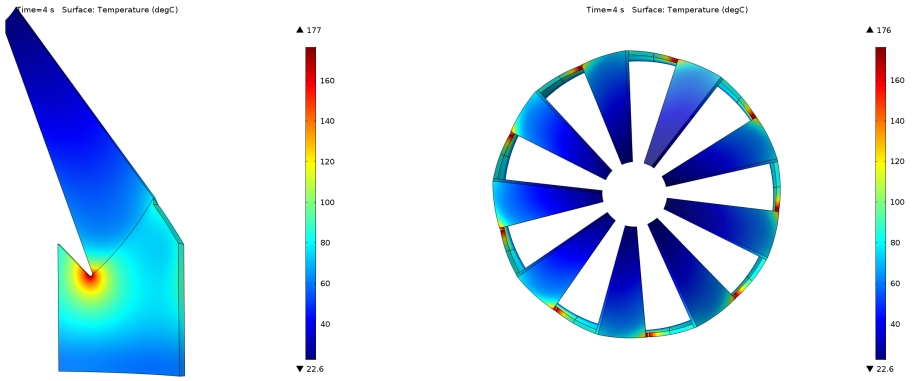

(a) 40° slice of the mixer (b) The full mixer, seen from above

Figure 46: Heating profile after 4 seconds of heating.

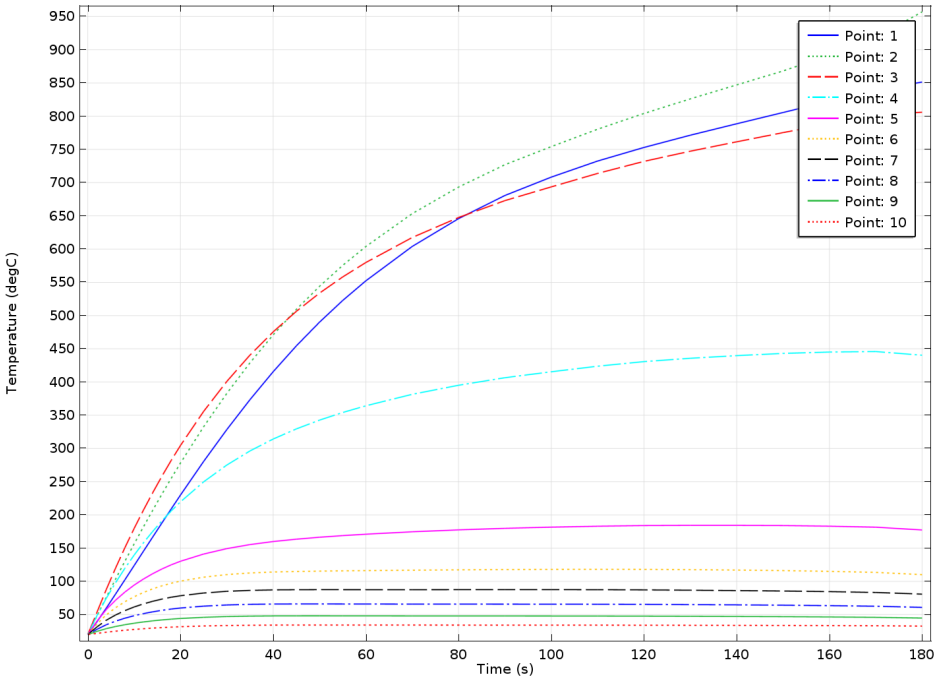

Figure 47: Graph of temperature over time in the measuring points.

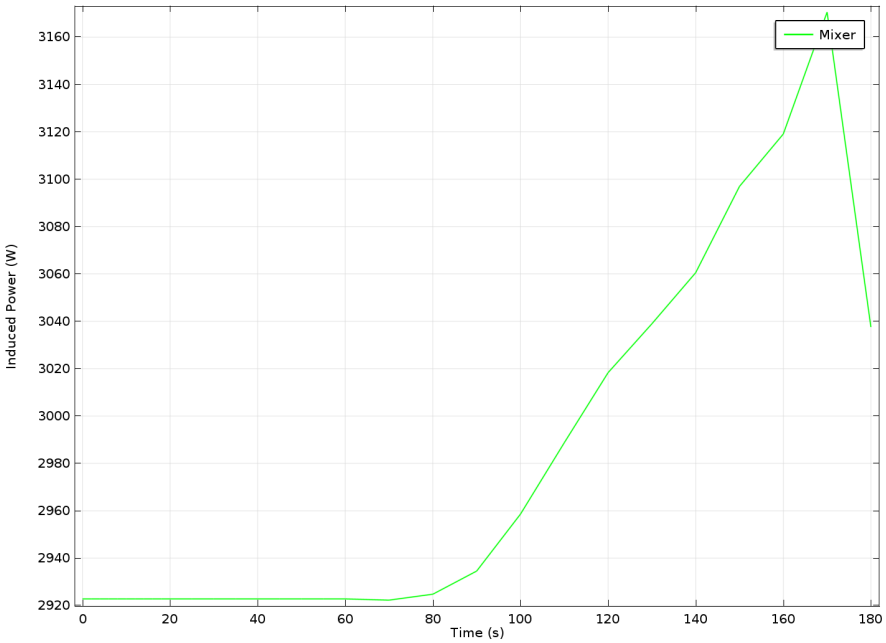

Figure 48: Graph of the induced power in the mixer.

From figure 46a it can be seen that the sharp corner at the bottom of the mixer blade received a strong heating. The hottest part of the mixer had reached 177° after 4 seconds. As can be seen in figure 47 measuring point 3 reached the highest temperature of the measuring points at over 950° after 180 seconds. The induced power in the mixer for the first 80 seconds was around 2920 W after that it increased until a total of 170 seconds had passed where it peaked at over 3160 W. This can be seen in figure 48.

5.3.2 Mixpipe 4

The result of the simulation using Mixer 3 with Mixpipe 4 is shown below. Figure 49 shows the temperature after 4 seconds and in figure 50 the temperature after 20 seconds. Figure 51 shows the graph over the temperature measured in the measuring points of the mixer. Seen in figure 52 is the induced power in the mixer and mixpipe.

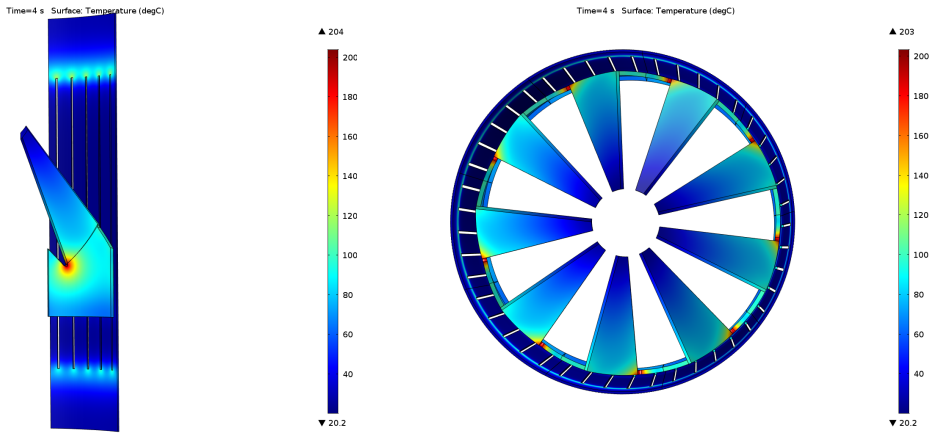

(a) 40° slice of the mixer (b) The full mixer, seen from above

Figure 49: Heating profile after 4 seconds of heating.

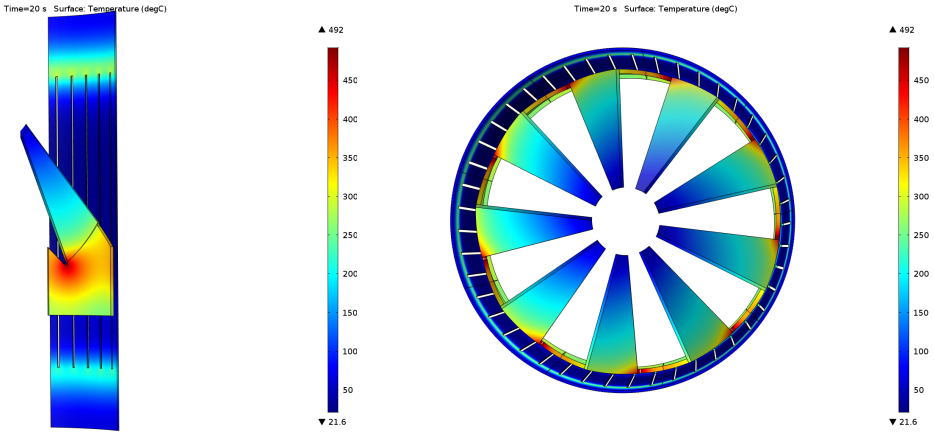

(a) 40° slice of the mixer (b) The full mixer, seen from above

Figure 50: Heating profile after 20 seconds of heating.

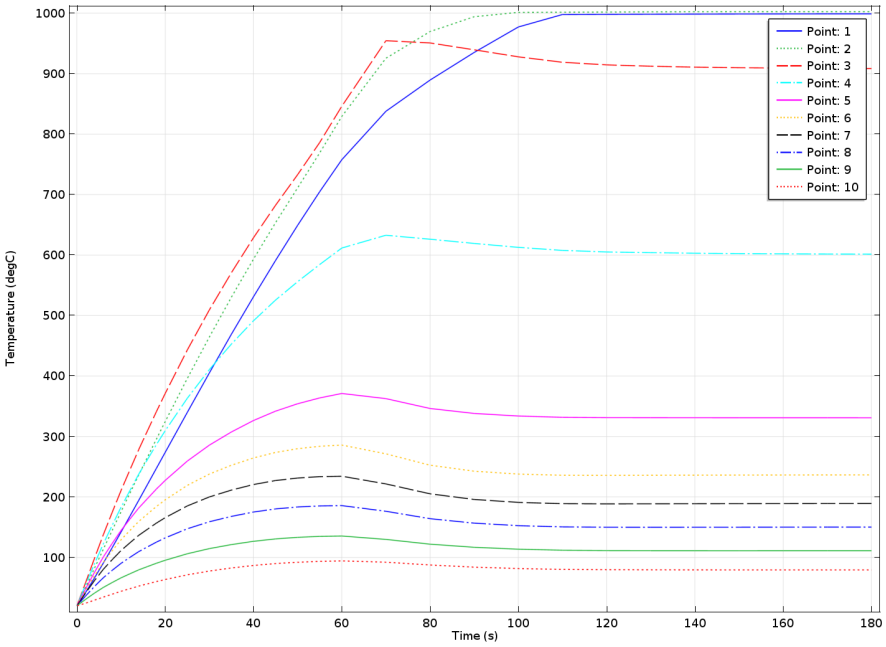

Figure 51: Graph of temperature over time in the measuring points.

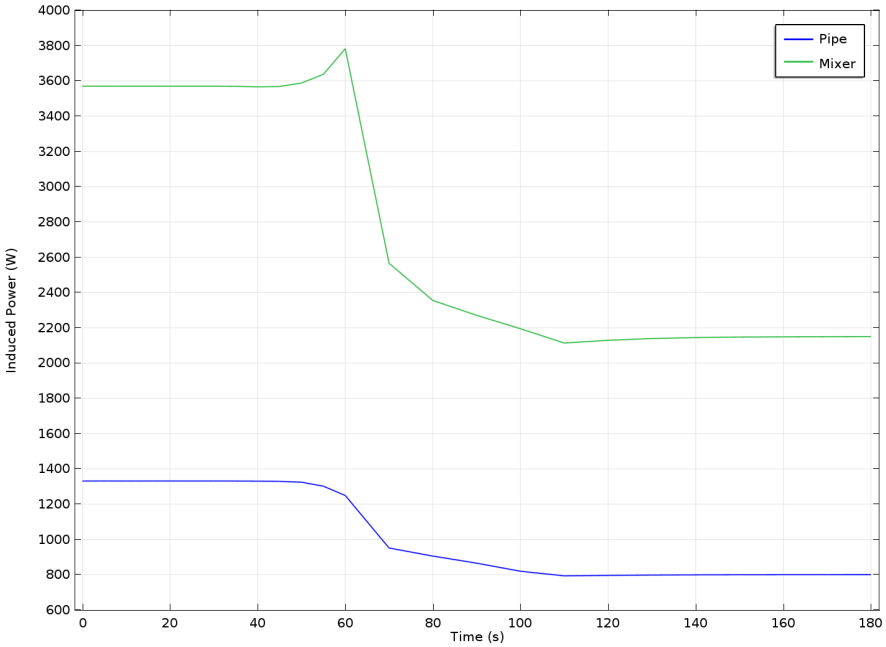

Figure 52: Graph of the induced power in both mixer and mixpipe.

In figures 49a and 50a it can be seen that the mixpipe was heated the most at the corners of the slits and that the top corners were heated more than the bottom corners. It can also be observed from both figures that the sharp corner located at the bottom of the mixer blade had the highest temperature of the model. From figures 49a and 50a it can be seen that the mixer blades received a notable heating where the part of the mixer blade located closest to the windings increased the most in temperature. As can be seen in figure 51 measuring points 1, 2 and 3 increased the most in temperature and after 180 seconds they had all reached temperatures of over 900°C. As can be seen in figure 52 the induced power in the mixer was slightly below 3600 W in the beginning of the simulation and it peaked after 60 seconds with 3800 W then decreased and after 180 seconds reached about 2200 W. The induced power in the mixpipe was slightly above 1300 W the first 50 seconds, it then decreased and stayed at about 800 W between 120 seconds and 180 seconds.

5.3.3 Mixpipe 5

The result of the simulation using Mixer 3 with Mixpipe 5 is shown below. Figure 53 shows the temperature after 4 seconds, in figure 54 is the graph over the temperature measured in the measuring points of the mixer, and in figure 55 is the induced power in the mixer and mixpipe.

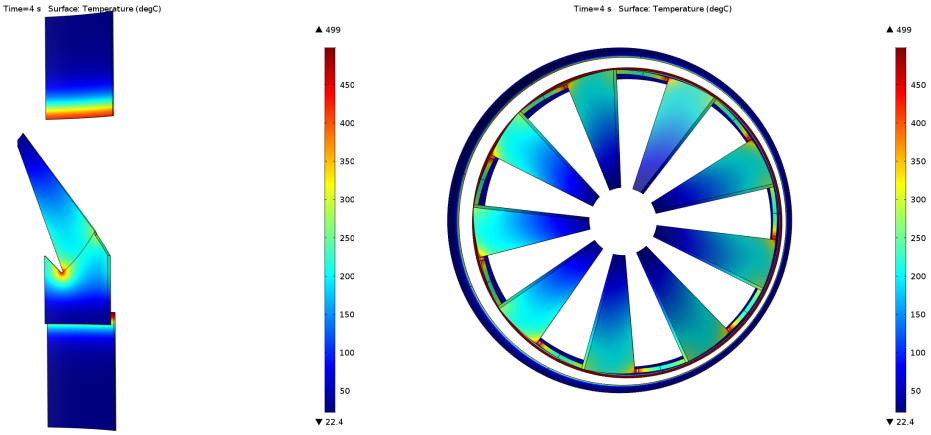

(a) 40° slice of the mixer (b) The full mixer, seen from above

Figure 53: Heating profile after 4 seconds of heating.

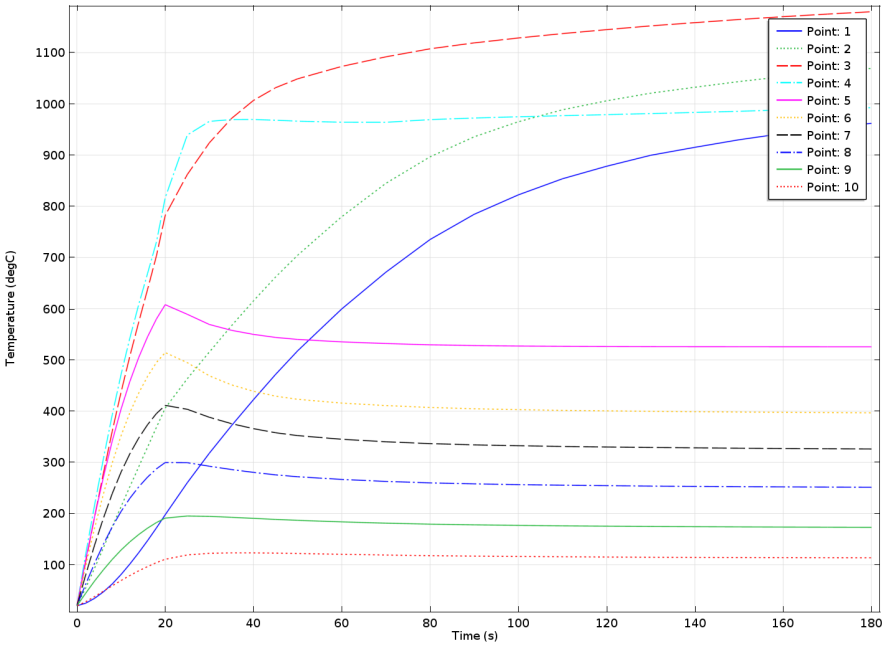

Figure 54: Graph of temperature over time in the measuring points.

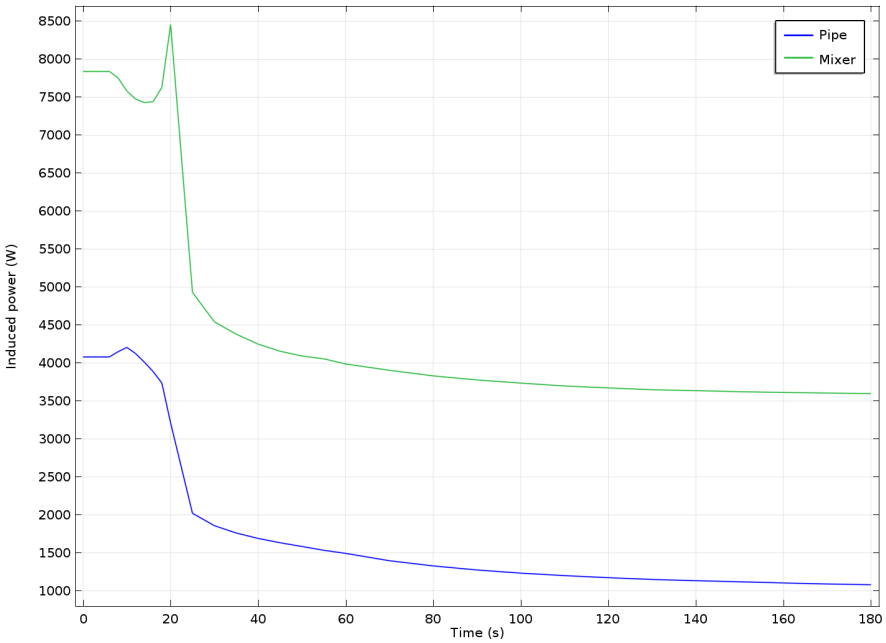

Figure 55: Graph of the induced power in both mixer and mixpipe.

As can be seen in figure 53a after 4 seconds the highest temperature of the mixpipe was found at the edges of the cut out, close to the windings. The highest temperature of the mixer was found at the sharp corner at the bottom of the mixer blade. The top part of the mixer wall along with the bottom part of the mixer blade was heated more than the bottom half of the mixer wall. Looking at figure 53b it can be seen that the entire mixer blade except for the end of the blade reached temperatures of over 100°C after 4 seconds. Looking at figure 54 it can be seen measuring points 1 to 4 all reached temperatures of over 900°C. The measuring points placed in the blade all increased in temperature until 20 seconds where points where points 5 to 8 had a decline to stabilize a bit lower than their peak temperature. In figure 55 it can be seen that the induced power in the mixer had a local minimum at around 15 seconds and a maximum at 20 seconds. The maximum at 20 seconds reached almost 8500 W, after 20 seconds the induced power kept decreasing for the rest of the simulation. The mixpipe had a maximum induced power at around 10 seconds where about 4250 W was induced in the mixpipe. After the maximum the induced power in the mixpipe kept decreasing for the rest of the simulation.

5.4 Mixer 4

Shown below is the simulation of Mixer 3 run without a mixpipe. Figure 56 shows the mixer temperature after 4 seconds, in fugre 57 are the temperatures from the measuring points in the mixer and in figure 58 is a graph of the induced power in the mixer.

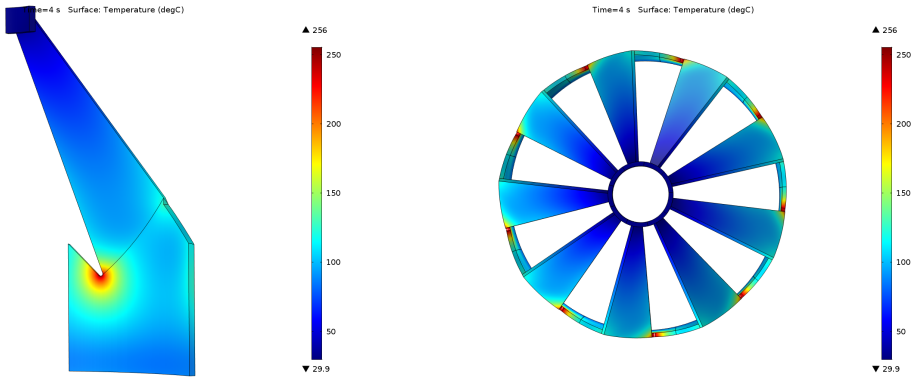

(a) 40° slice of the mixer (b) The full mixer, seen from above

Figure 56: Heating profile after 4 seconds of heating.

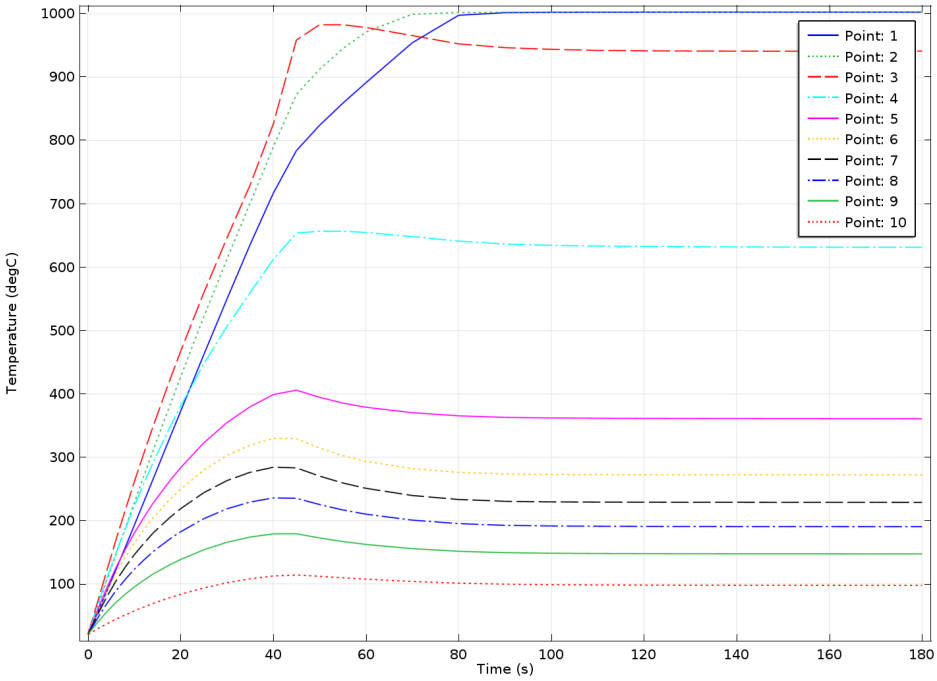

Figure 57: Graph of temperature over time in the measuring points.

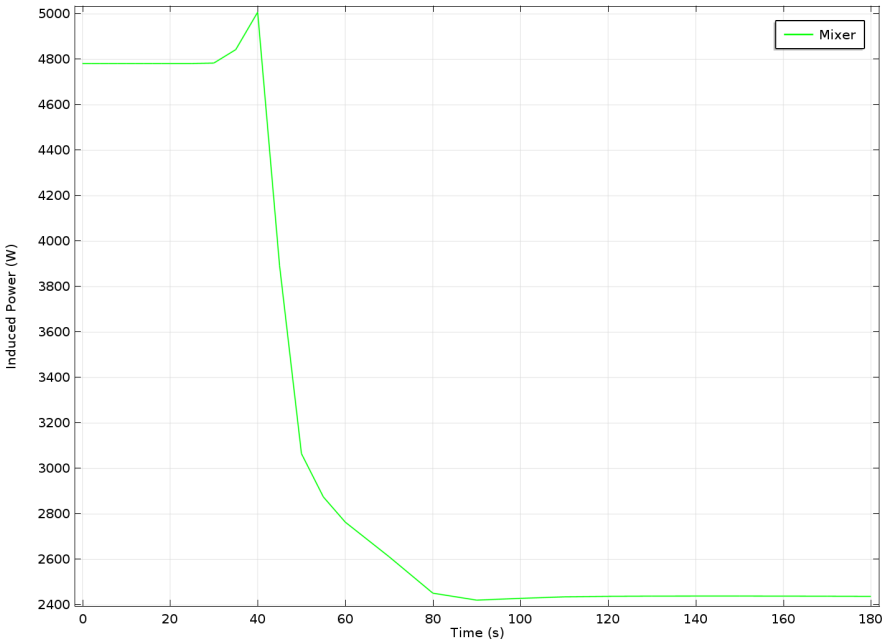

Figure 58: Graph of the induced power in the mixer.

As can be seen in figure 56a the highest temperature of the mixer was 256°C. The bottom part of the mixer wall was heated less than the top part of the mixer wall, and the sharp corner where the mixer blade was attached to the mixer wall had a strong local heating. From figure 57 it can be seen that measuring points 1 and 2 were heated the most and they both reached 1000°C. Figure 58 shows that the induced power in the mixer initially was about 4800 W. After 40 seconds the induced power peaked at about 5000 W and after that the induced power decreased to slightly over 2400 W.

5.4.1 Mixpipe 4

The result of the simulation using Mixer 4 with Mixpipe 4 is shown below. Figure 59 shows the temperature after 4 seconds, and in figure 60 is the graph over the temperature measured in the measuring points of the mixer. Shown in figure 61 is the induced power in the mixer and mixpipe.

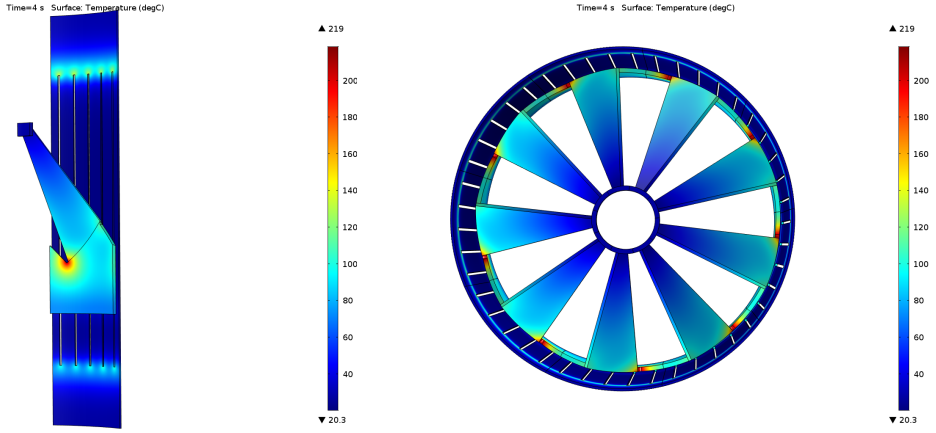

(a) 40° slice of the mixer (b) The full mixer, seen from above

Figure 59: Heating profile after 4 seconds of heating.

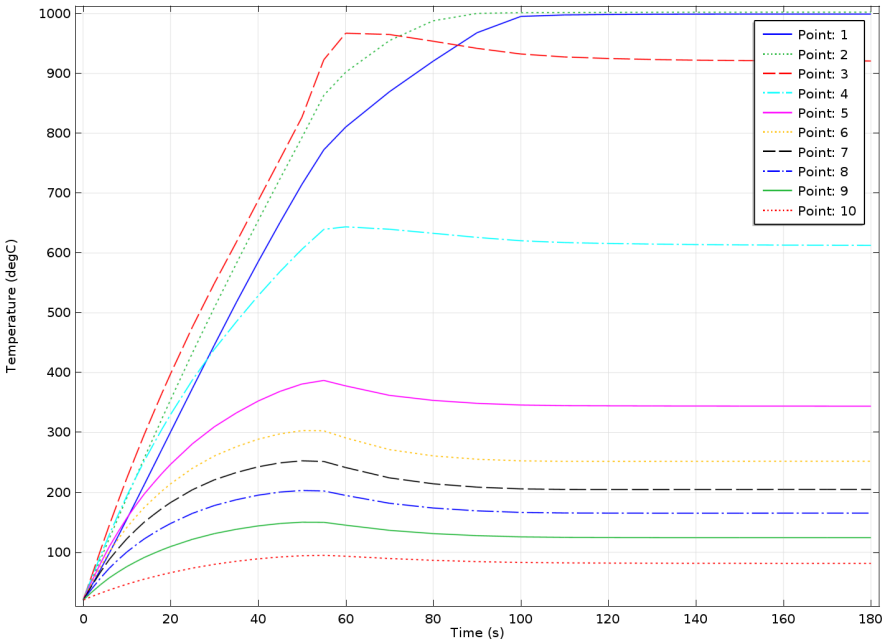

Figure 60: Graph of temperature over time in the measuring points.

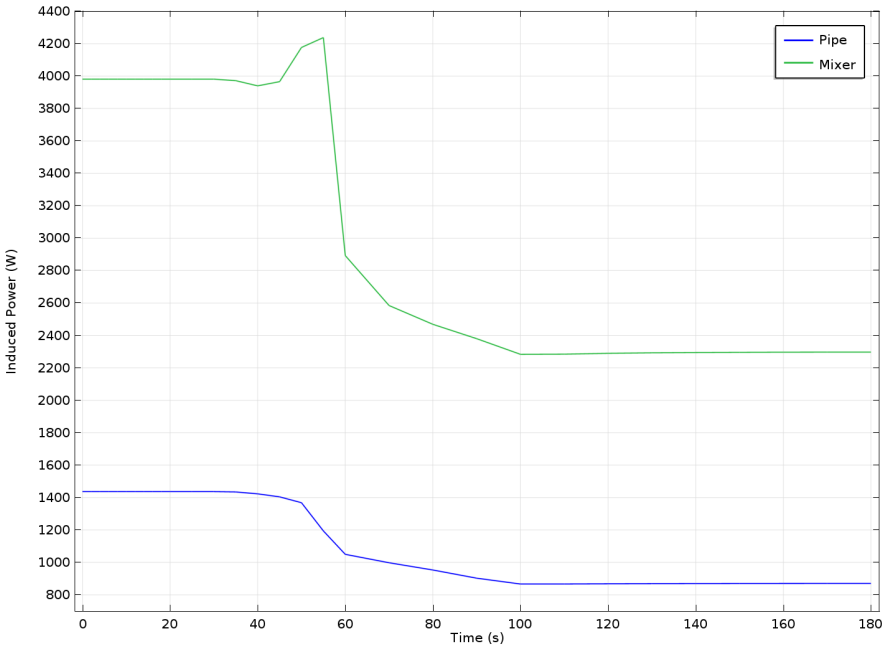

Figure 61: Graph of the induced power in both mixer and mixpipe.

As can be seen in figure 59a the heating of the mixpipe was mostly con-

centrated around the upper slit corners. The lower corners of the slits were also heated but the heating was less spread out than for the upper corners. The mixer received a strong local heating around the sharp corner at the bottom of the mixer blade and the lower part of the mixer wall was heated less than the upper part of the mixer wall. Looking at figure 59b it can be seen that the mixer blades were more heated outwards where they were closer to the mixpipe and windings. From figure 60 it can be seen that measuring point 3 remained the hottest until around 70 seconds where measuring point 2 and later also 1 surpassed it. Measuring points 1, 2 and 3 were all heated to above 900°C. As can be seen in figure 61 the induced power in the mixer was almost 4000 W the first 40 seconds with a local minimum at 40 seconds. After the first 40 seconds the induced power in the mixer increased to 4200 W at 55 seconds it started decreasing. At the end of the simulation the induced power in the mixer was about 2300 W. The induced power in the mixpipe started at slightly above 1400 W and began decreasing at 35 seconds.

5.4.2 Mixpipe 5

The result of the simulation using Mixer 4 with Mixpipe 5 is shown below. Figure 62 shows the temperature after 4 seconds, in figure 63 is the graph over the temperature measured in the measuring points of the mixer, and in figure 64 the induced power in the mixer and mixpipe is shown.

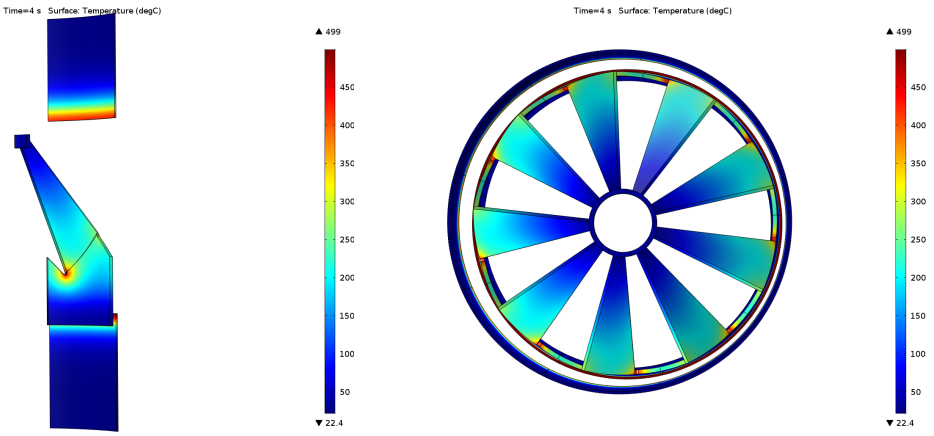

(a) 40° slice of the mixer (b) The full mixer, seen from above

Figure 62: Heating profile after 4 seconds of heating.

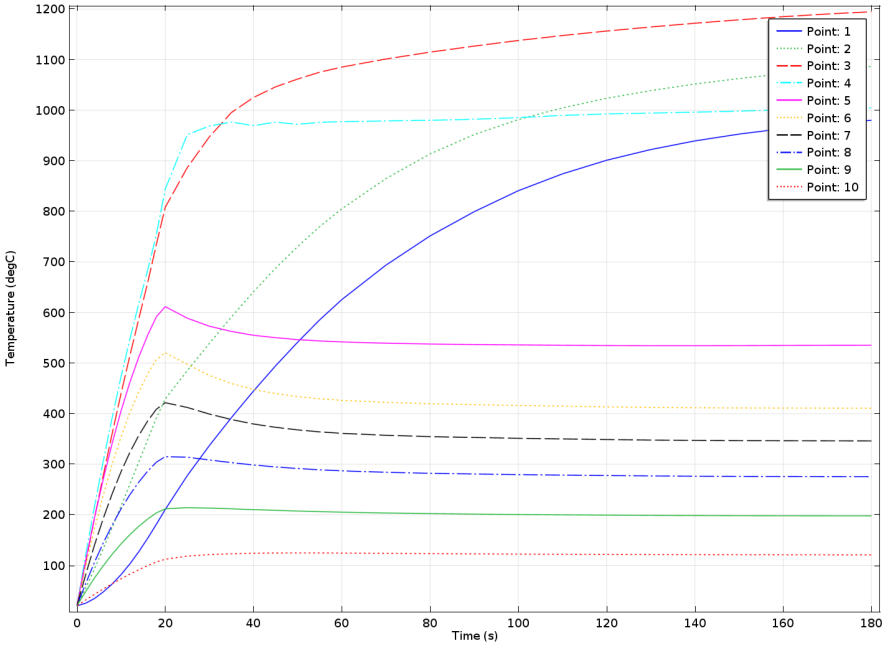

Figure 63: Graph of temperature over time in the measuring points.

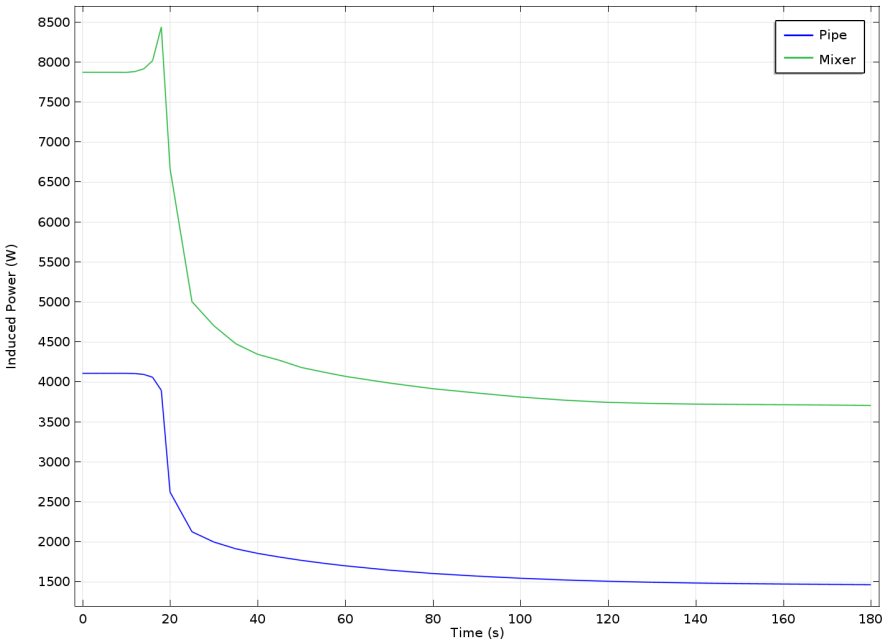

Figure 64: Graph of the induced power in both mixer and mixpipe.

From figure 62a it can be seen that the edges of the cut out closest to

the winding were heated the most of the mixpipe. The upper part of the mixer wall was heated more than the lower and the highest temperature in the mixer wall was found in the sharp corner where the bottom of the mixer blade was attached. As can be seen in figure 62b the blades were heated to above 100°C for most of the blade except the bits of the blade closest to the attached cylinder in the middle. Figure 63 shows that measuring points 1 to 4 were heated to over 900°C and that measuring point 3 was heated to almost 1200°C. As seen in figure 64 the induced power in the mixer peaked at 18 seconds followed by a steep decrease of induced power. The induced power in the mixpipe was initially slightly above 4000 W and started decreasing at 16 seconds. At 180 seconds the induced power of the mixpipe was less than 1500 W.

5.5 Mixer 5

Since Mixer 5 was directly attached to the mixpipe, unlike the other mixers, no simulations were run for Mixer 5 without a mixpipe.

5.5.1 Mixpipe 1

The result of the simulation using Mixer 5 with Mixpipe 1 is shown below. Figure 65 shows the temperature after 4 seconds, and in figure 66 is the graph over the temperature measured in the measuring points of the mixer. Seen in figure 67 is the induced power in the combined mixer and mixpipe.

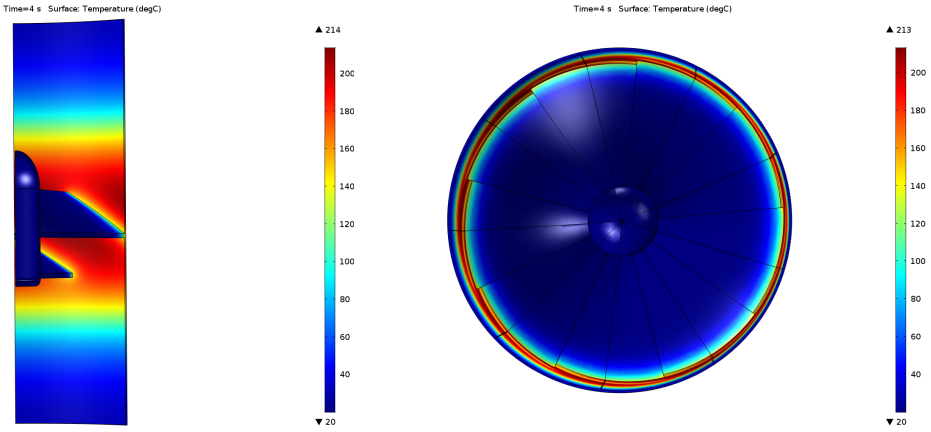

(a) 40° slice of the mixer (b) The full mixer, seen from above

Figure 65: Heating profile after 4 seconds of heating.

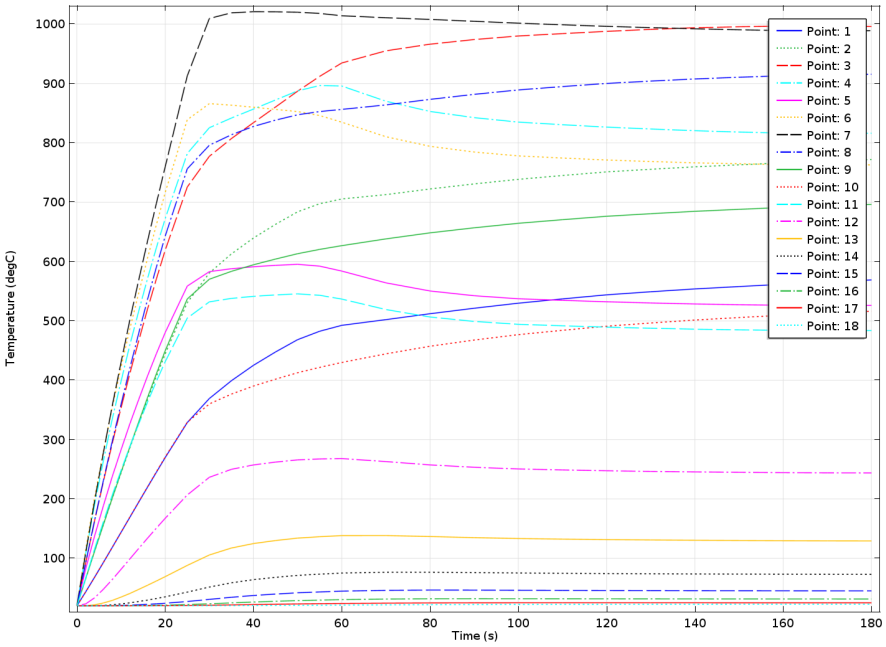

Figure 66: Graph of temperature over time in the measuring points.

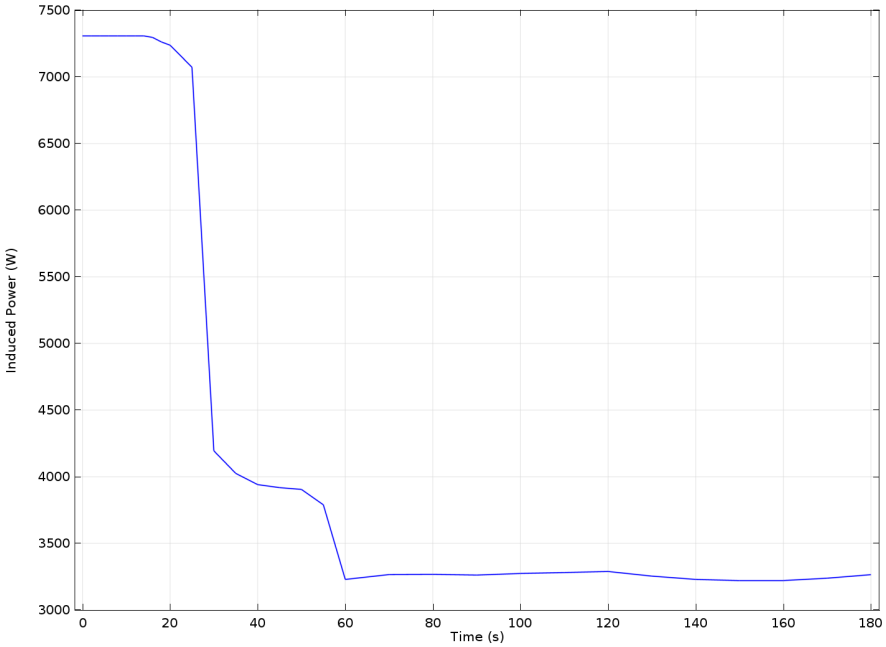

Figure 67: Graph of the induced power in the mixpipe.

From figure 65 it can be seen that the mixpipe was evenly heated around the pipe, except where the mixer blades were attached to mixpipe resulting in a lower temperature of the pipe. Looking at figure 65b it can be seen that the piece in the middle of the mixer had received low or no heating and that the mixer blades were only heated close to the pipe wall after 4 seconds. In figure 66 it can be seen that measuring points 3 and 7 reached the highest temperature at around 1000°C. From figure 67 it can be seen that the induced power initially was about 7250 W and that the induced power dropped fast at 25 seconds and 55 seconds. Between 60 seconds and 180 seconds the induced power had some variations around 3250 W.

5.5.2 Mixpipe 4

The result of the simulation using Mixer 5 with Mixpipe 4 is shown below. In figure 68 the temperature after 4 seconds is shown, in figure 69 is the graph over the temperature measured in the measuring points of the mixer and in figure 70 the induced power in the combined mixer and mixpipe.

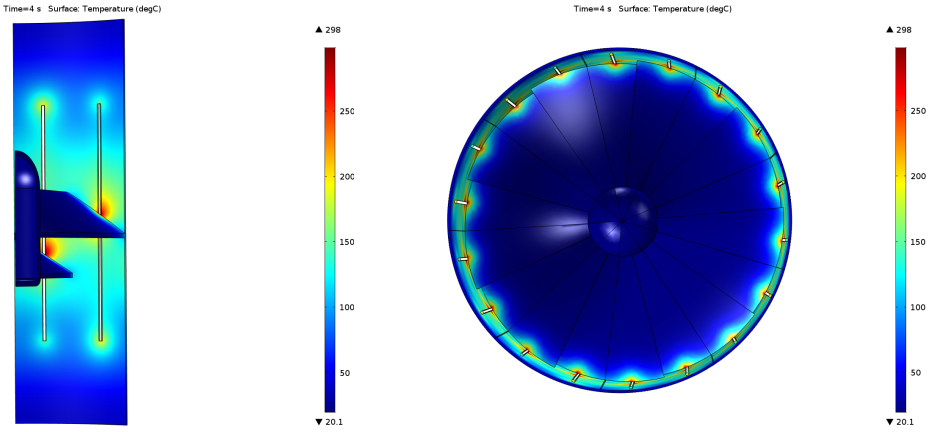

(a) 40° slice of the mixer (b) The full mixer, seen from above

Figure 68: Heating profile after 4 seconds of heating.

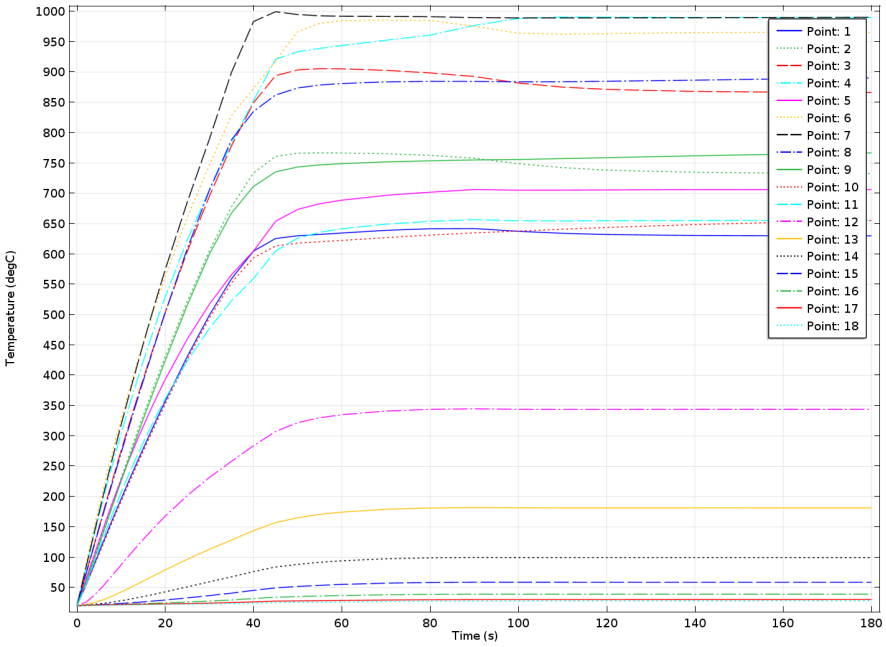

Figure 69: Graph of temperature over time in the measuring points.

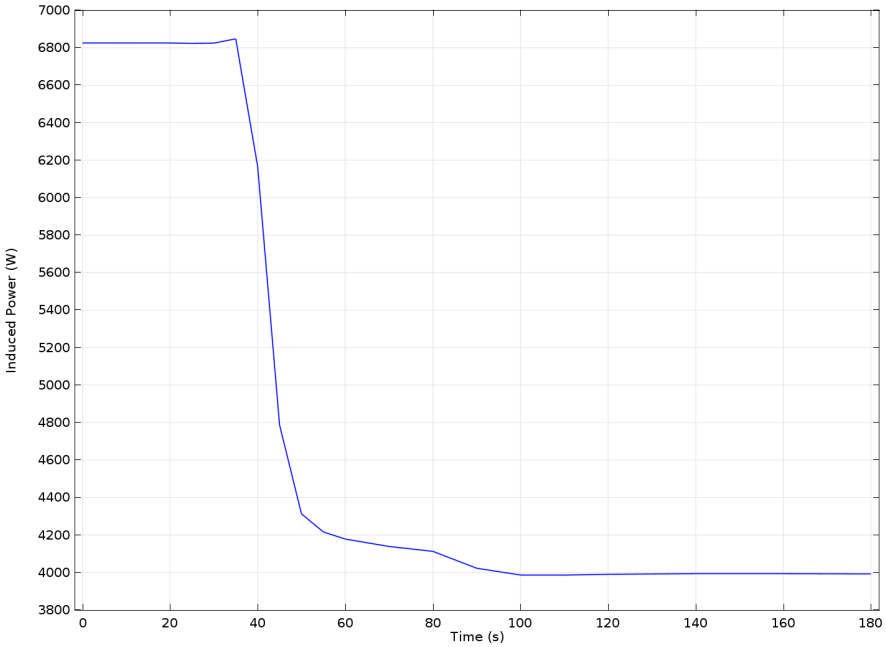

Figure 70: Graph of the induced power in the mixpipe.

In figure 68a it can be seen that the mixpipe received the most heating at the slits where the mixer blades are also attached as well as a strong heating effect at the corners of the slits. From figure 68b it can be seen that the the heating of the blades reached closest to the center of the mixer at the places where the blades were attached around the mixpipe slits. As can be seen in figure 69 the measuring points that were heated the most were points 7 and 4 which both reached around 1000° C. As can be seen in figure 70 the induced power was slightly above 6800 W between 0 seconds and 60 seconds. Between 35 seconds and 100 seconds the induced power decreased and after 100 seconds the induced power was 4000 W.

5.6 Improved models

This section includes some variations and improvements in order to handle some of the warm spots in the previous designs which was a problem for the designs to be plausible for practical use.

5.6.1 Analysis of slits

By analysing the corners of the slits of the mixpipe it's possible to see partly why the the local warm heating occurs by the edges of the slits. A model of

the slits was used to simulate current passing the corner and to demonstrate the effects of the geometry. Figure 71 shows a regular slit with sharp corners and figure 72 shows the result of a slit with the corners rounded off.

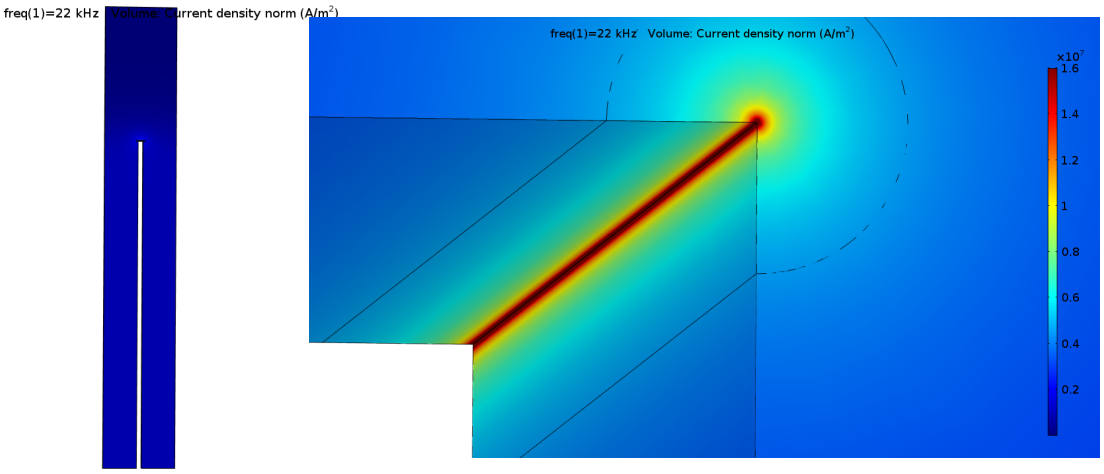

(a) The whole model

(b) Zoomed in on the right corner

Figure 71: Simulation of the sharp edges of the slits

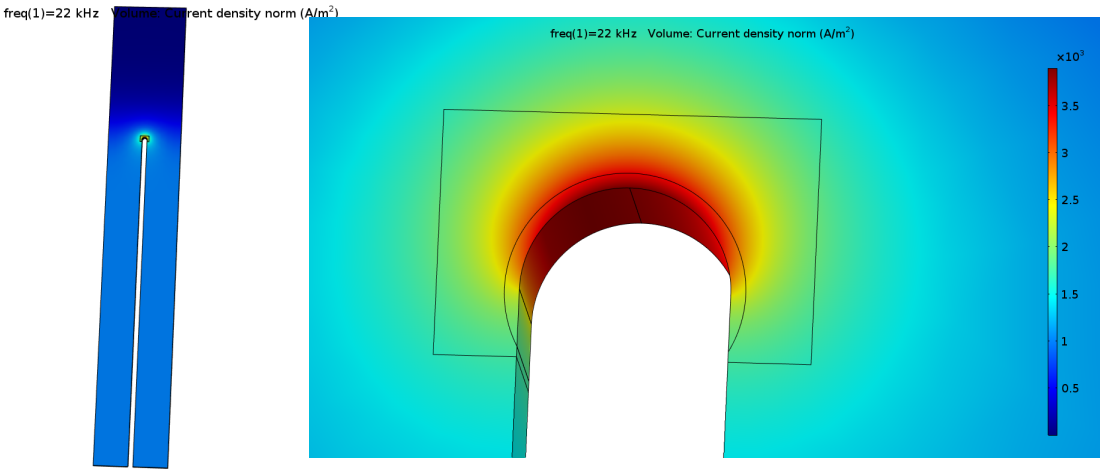

(a) The whole model

(b) Zoomed in on the corner

Figure 72: Simulation of the rounded edges of the slits

As can be seen in figure 71 the current is concentrated in a small point at the edge of the corner. Compared to figure 72 where the current is more spread out, resulting in lower current concentration and heat generated at the corner.

5.6.2 Mixer 1.1 Mixpipe 5

In an effort to solve the local warm spots forming at the corners by the lower edge of the mixer blade the corners were rounded off. The design was then simulated using identical settings to Mixer 1 Mixpipe 5.

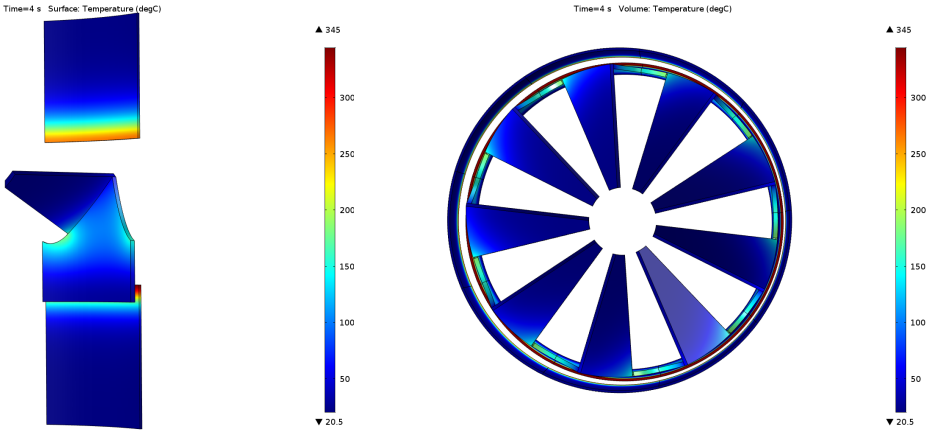

(a) 40° slice of the mixer (b) The full mixer, seen from above

Figure 73: Heating profile after 4 seconds of heating.

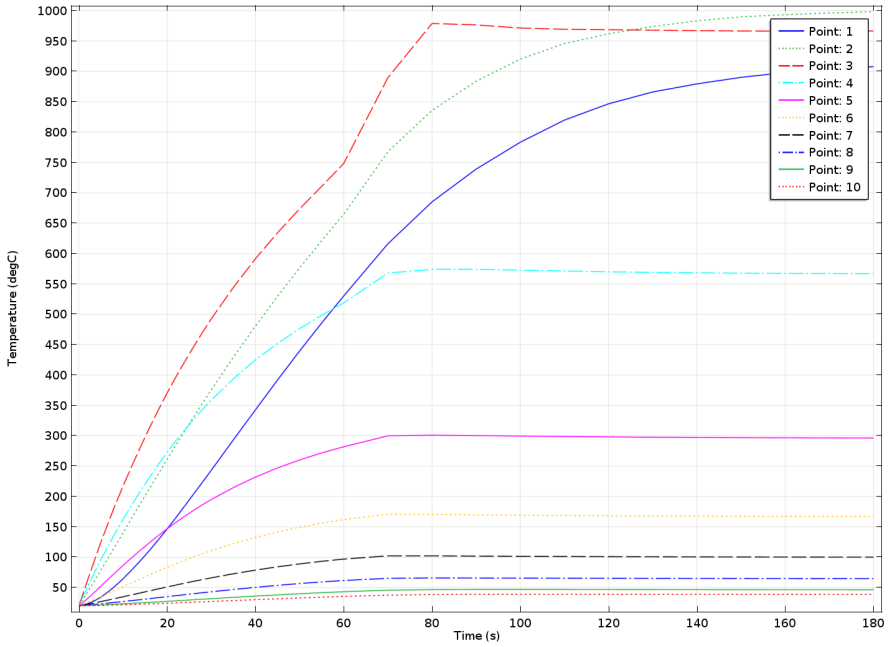

Figure 74: Graph of temperature over time in the measuring points.

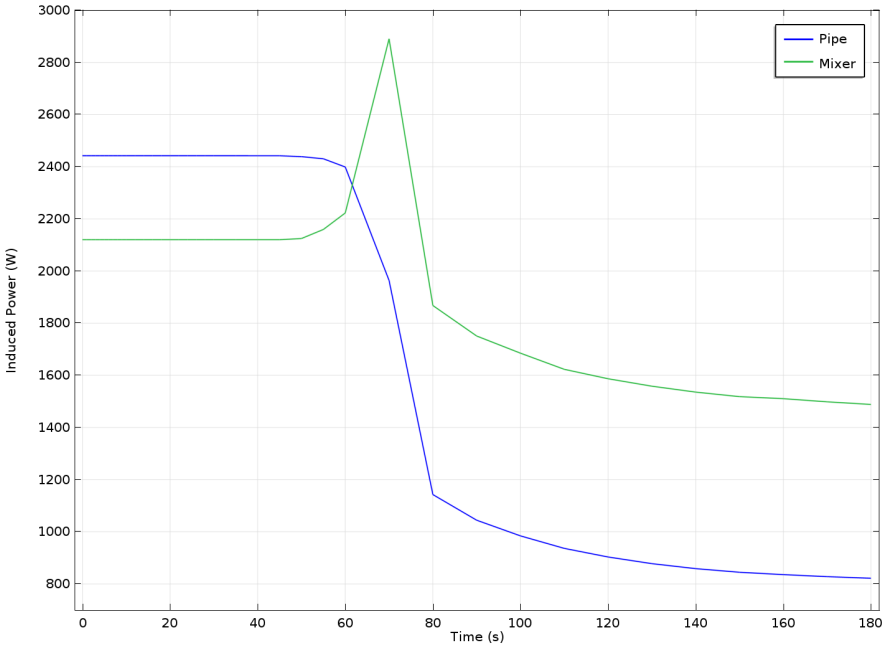

Figure 75: Graph of the induced power in both mixer and mixpipe.

Figure 73 shows how the most heating is induced by the sharp corner at the lower part of the mixer blades, reaching about 150°C after 4 seconds. As can be seen in figure 74 the temperature in measuring point number 3 rises in 80 seconds to almost 1000° with an induced power of about 2150 W up until reaching the curie temperature after approximately 60 seconds. Figure 75 shows the induced power in the mixer and mixpipe.

5.6.3 Mixer 3 Mixpipe 4 with winding gap

In an effort to solve the problem with the warm spot forming by the lower edge of the mixer blade another simulation was run with the two windings closest to the warm spot removed.

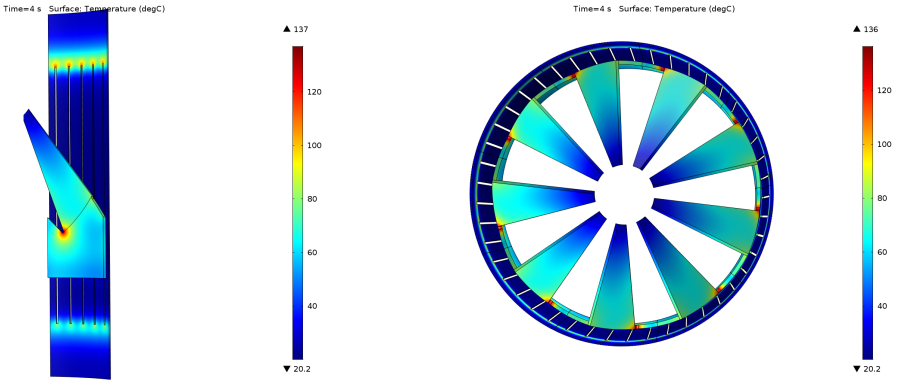

(a) 40° slice of the mixer (b) The full mixer, seen from above

Figure 76: Heating profile after 4 seconds of heating.

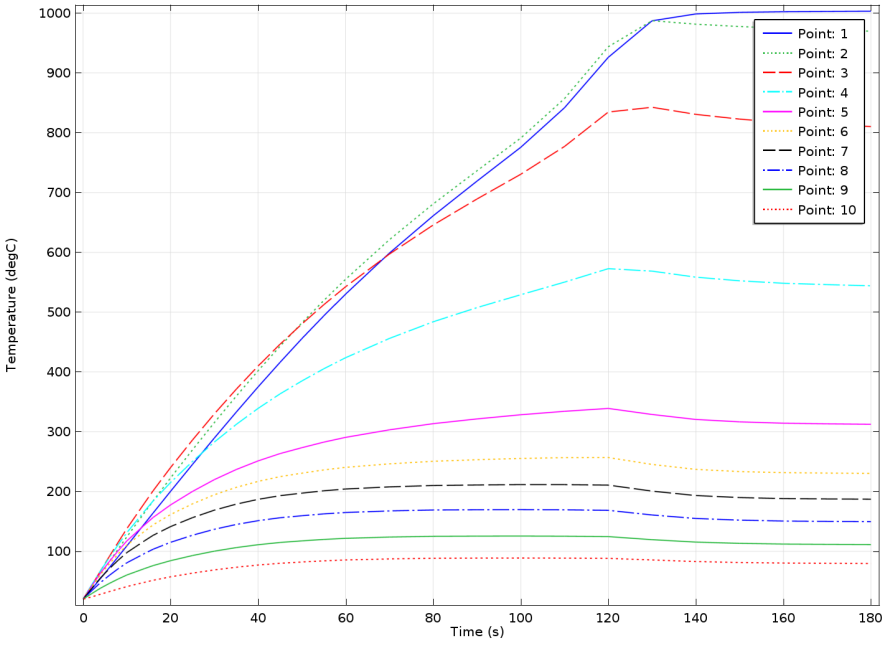

Figure 77: Graph of temperature over time in the measuring points.

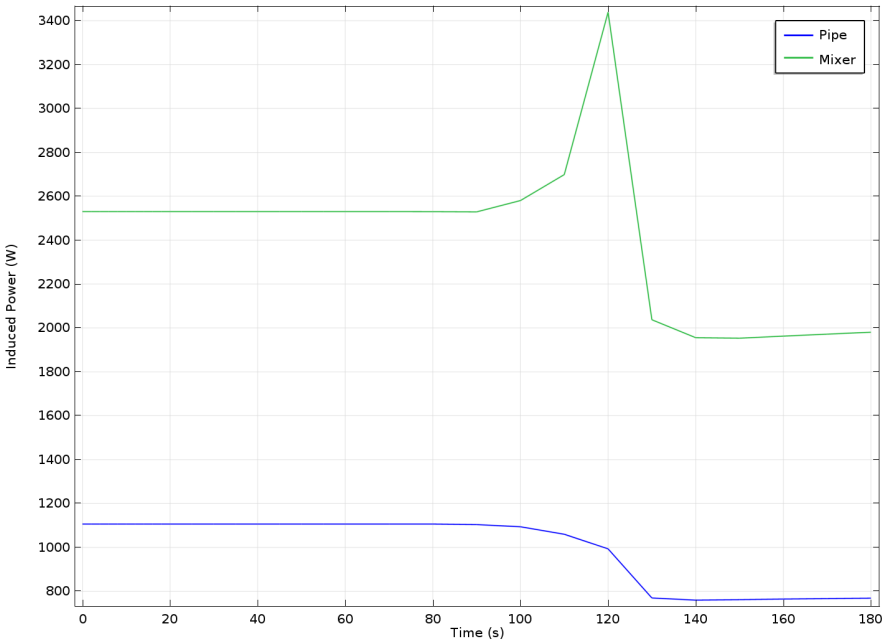

Figure 78: Graph of the induced power in the mixpipe.

Figure 76 shows the results of Mixer 3 Mixpipe 4 with the warm spot reaching 137°C after 4 seconds. As can be seen in the figure the warm spot isn't gone but it shows a large reduction of heating generated in that spot. Figure 78 shows a induced power of over 2500 W for the first 90 seconds, then reaching a peak power of over 3400 W before sharply dropping to about 2000 W. Looking at figure 77 shows that the temperature of many of the measuring points along the blade reach a somewhat stable temperature after about 60 seconds.

6 Validation

In addition to the simulation models a real size prototype was built to run real life tests on. In this section the building of the model, the test setup and the result of the tests will be presented.

6.1 Construction

The selected mixer to build was Mixer 3 and the selected mixpipe was Mixpipe 4 as that combination both gave good results and the actual construction seemed manageable. The mixer was made of a 2 mm thick sheet of ferritic stainless steel EN 1.4016 which was laser cut. The design for the mixer laser cut can be seen in figure 79. The final mixer cut had an additional cut at the bottom of the mixer blade to more easily be able to bend the blade, The additional cut can be seen in figure 81.

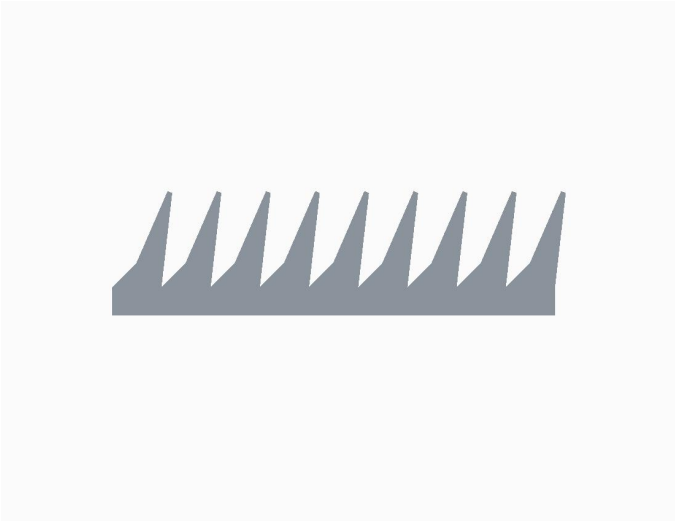

Figure 79: Mixer cut out

The mixpipe was made of a 1 mm thick sheet of austenitic stainless steel EN 1.4404 which was laser cut. The design for the mixpipe laser cut can be seen in figure 80

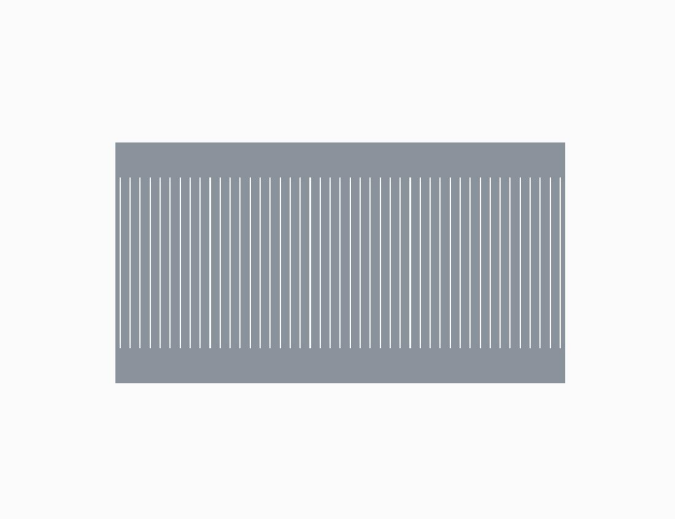

Figure 80: Mixpipe cut out

With the stainless steel cut the mixer piece was bent so that the ends touched and then welded together. The cuts at the bottom of the mixer blades were then melted together. A finished mixer, before the melting of the cuts, can be seen in figure 81 below.

Figure 81: Mixer with visible blade cuts

After the ends had been welded together the mixer blades were bent until they were angled approximately 45° inwards. With the mixer constructed the mixpipe was bent until the ends touched. The bent mixpipe, before the mixer was mounted, can be seen in figure 82 below.

Figure 82: Mixpipe before mounting of mixer

The mixer was then placed inside of the mixpipe with a layer of Superwool between to insulate the pieces from each other. The mixpipe was then brazed together. Both the mixer and mixpipe were then painted black to allow for the IR-camera to take as accurate pictures as possible.

To construct the windings a wooden template was made to wind the windings around. The windings were made out of copper tubing intended for brake fluid for cars. The copper tubing was wound around the wooden template and the excess tubing other than the 21 windings was straighted out to have fittings placed on for the power supply and cooling water. The windings still around the wooden template can be seen in figure 83 below

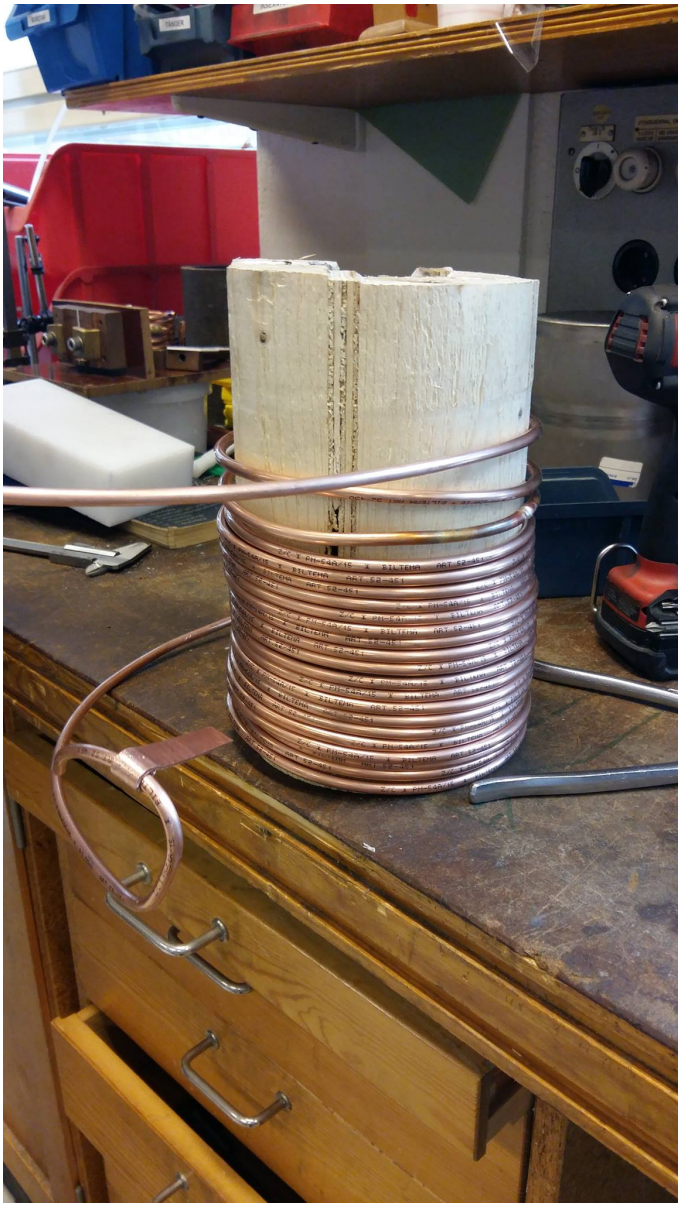

Figure 83: Windings still around the wooden template

The fitting for the power supply was made of a copper sheet with one end bent to fit around the copper tubing and the other end with a hole through which a bolt could be fitted to attach to the power supply. The power supply fittings are shown in figure 84 below.

Figure 84: Power supply fittings brazed on to the copper tubing

The cooling fitting was made out of a pipe seal with a drilled hole which fitted on the copper tube. On the other side of the pipe seal a hose connection was screwed on. Both the fittings for the power supply and the cooling supply were brazed on to the copper tubing. The windings were then fitted around the mixpipe with a layer of Superwool between windings and mixpipe to isolate them from each other. Every turn of the winding was then taped with kapton tape on one side to isolate the turns from each other. The windings

taped and mounted around the mixpipe are shown in figure 85 below.

Figure 85: Windings mounted around the mixpipe

The copper tubing leading from the windings to the fittings was then taped with electrical tape and the two pieces of tubing were twinned around each other to reduce the inductance they added to the circuit. Three wooden racks were then constructed and strapped around the windings to keep them from moving. One of the mounted wooden racks can be seen in figure 86

below and the full build of the model can be seen in figure 87.

Figure 86: One of the mounted wooden racks

Figure 87: Full build of the test piece

With everything mounted the impedance and inductance of the piece was measured at 20 kHz. The inductance was measured to 42 μH and the impedance to 1.5 Ω

6.2 Test runs and results

The copper windings were connected to a water source to use as cooling and to a power supply. The power supply fed the windings with 81.2 A RMS at a frequency of 22 kHz. Power was the supplied for up to 25 seconds to the test piece which started the test at room temperature. The heating of the mixer was recorded with an IR-camera. The IR-camera worked using two temperature intervals. The first interval worked for temperatures up to 350° C and the second interval worked for temperatures of 200° C - 1200° C. Every test run thus had to be done twice, once for each interval, in order to receive data for the entire heating process. The images from the camera were extracted as a matrix with the temperature value for each pixel of each frame, along with a vector which contained timestamps for the frames. The two image sequences of each run were then matched and merged with updated timestamps.

Below are images taken from the IR-camera. Figures 88 and 89 are taken with the mixer blades pointing toward the IR-camera. Figures 90 and 91 are taken at a slight angle with the mixer blades pointing away from the IR-camera.

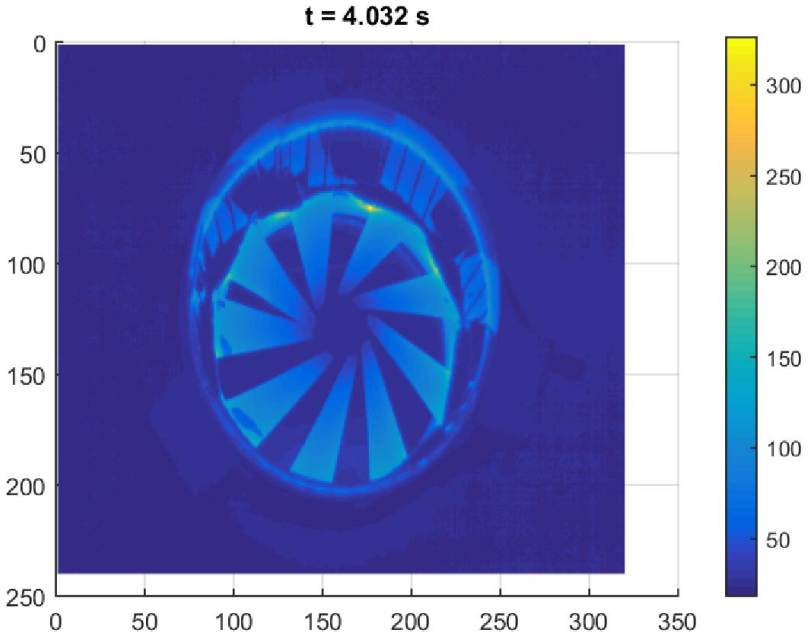

Figure 88: Test piece after 4 seconds of heating

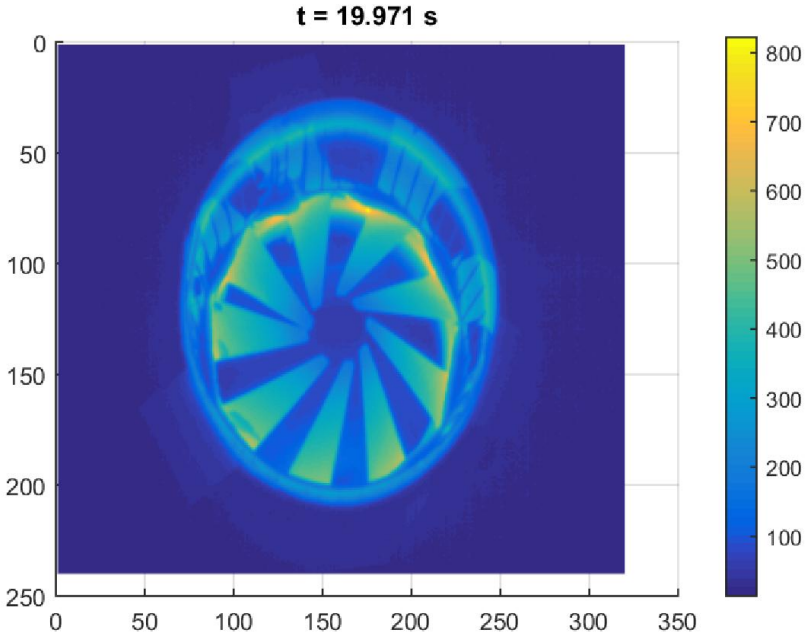

Figure 89: Test piece after 20 seconds of heating

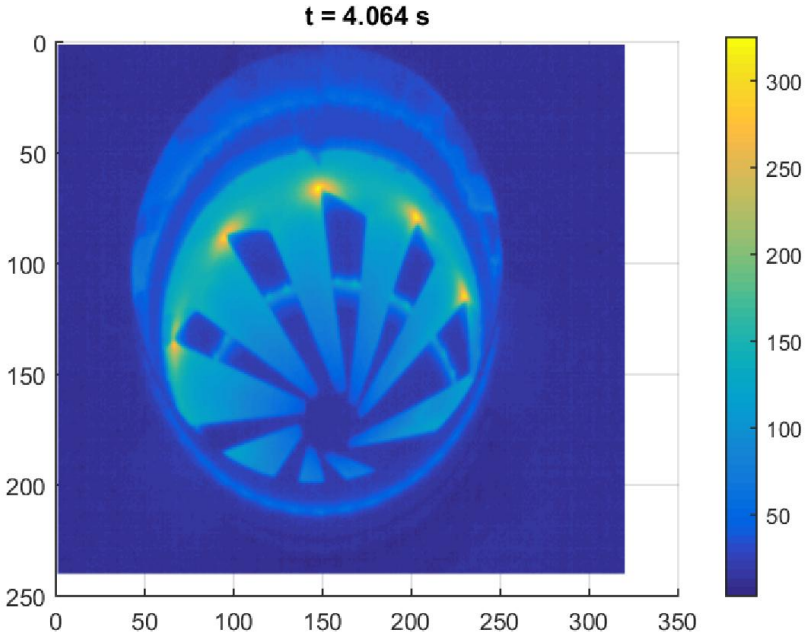

Figure 90: Test piece after 4 seconds of heating

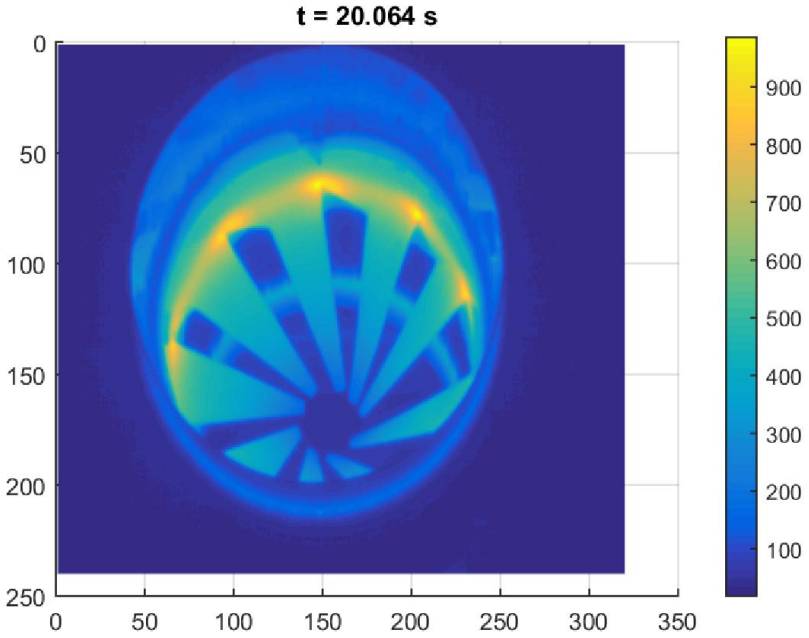

Figure 91: Test piece after 20 seconds of heating

In figures 88 and 90 it can be seen that after 4 seconds of heating the sharp bottom corner where the mixer blade is attached to the mixer wall has received strong heating effect. From figures 89 and 91 the heated belts at the corners of the mixpipe slits can be seen . In figure 89 the band can be seen above the mixer and in figure 91 the band was below the mixer as the mixer was pointing in opposite directions in these figures. In figure 91 it can be seen that the mixer wall is heated more the closer to the mixer blade it is. The bottom of the mixer wall, which here is directed upwards, had not received as much heating.

7 Analysis and discussion

7.1 Mixers

Judging by the results of the simulations it becomes apparent that the design of the mixer has a great impact on the performance. In order to achieve as good heat transfer as possible it's important to induce power along the mixer blades because the blades has a much higher heat transfer coefficient due to the airflow through the pipe. Ideally all power should be induced in the mixer blades but realistically this becomes a challenge. In Mixer 1 and Mixer 2 the blades are partly shielded by the wall of the mixer resulting in almost all power induced in the wall of the mixer instead of the mixer blades. The lower heat transfer coefficient of the mixer wall results in a rather slow heat buildup in the mixer up until reaching the curie temperature, which leads to a drastic efficiency drop allowing temperature to reach a stable state and can be seen in figures 16 and 35. In this mixer almost all energy in the blades are the result of heat conducting from the wall, and not directly induced. This process is not nearly quick enough for the intended application to heat the exhausts within seconds. Also, all surface area parallel to the windings, which is important for efficient inductive coupling, is limited to only the wall of the mixer, greatly limiting the possible amount of induced power. This results in a rather inefficient coupling and a overall under performing solution.
In comparison with Mixers 1 and 2, Mixers 3 and 4 improve on several of these key areas. By angling the mixer blades upward and extending them as done in Mixer 3 and 4 the surface area parallel to the windings is increased substantially leading to increased induced power, and importantly power is induced further out in the mixer blades. The increased induced power can be seen in figure 46 where the new design has a almost 50% improvement over Mixer 1 shown in figure 15 with the same number of windings. These graphs also illustrate how Mixer 3 can be run efficiently for a longer time, due to more of the power being induced in the blades which has a much greater heat transfer coefficient to the air, before reaching the curie temperature and dropping in efficiency.

The difference between Mixer 1 and 2 is an added inner ring with the intent of connecting one blade to another, possibly adding an additional path for the current to flow. In the same way an inner ring was added to Mixer 3, resulting in Mixer 4. By analyzing the graphs of induced power of the different mixers, figures 17 versus 36 and 45 versus 58, it's possible to conclude that the added ring offers a small increase in power. Although it's hard to tell if the difference is due to providing a path for the current to flow or simply because the ring added additional conducting surface area parallel

to the windings.

Each of the mixers show a clear problem, namely the warm spot created in the mixer wall corner by the lower part of the mixer blade. It is a problem that occurs in all the mixers and needs to be addressed for the designs to be plausible for actual use. There are several possible ways to approach this problem. One possible design change would be to round of the edges, as done in Mixer 1.1, causing less heating to occur as shown in section 5.6.2. Although, as can be seen when comparing figures 74 and 29 it can alleviate the problem somewhat but not enough to solve the problem. The second and a more effective way is to remove the windings closest to the warm spot. As can be seen in section 5.6.3 this method has the possibility to substantially reduce the heat generated in the warm spot, while still inducing almost the same amount of power in the blades where the power is most needed. A third and probably most effective way would be to use another mixer design altogether which doesn't have the deep cuts by the blade where the current is forced together.

Since Mixer 5 had a different design it did not experience the same problem with the warm corner in the mixer wall. Mixer 5 was designed with the intention to remove one layer of shielding from the blades of the mixer by removing the mixer wall and attaching the blades directly to the mixpipe. The result of this change were that with the combination of Mixer 5 and Mixpipe 1 the design relied entirely on heat transfer from the mixpipe which was deemed too slow to effectively heat the exhausts within seconds. With Mixer 5 Mixpipe 4 the idea of using Mixpipe 4 allowed the magnetic field to reach the blades, but Mixer 5 has too little surface area parallel to the windings to effectively induce power, and therefore still relied heavily on heat transfer to heat the blades. This mixpipe also introduced the problem of warm spots forming where the mixer blades bridges the gaps of the slits of the mixpipe. This is due to the blades providing a path for the current to flow from one side of the slit to another, resulting in high current concentrations. As stated before, the results shows that Mixer 5 can't heat the exhausts quickly enough and as such Mixer 5 design was discarded.

7.2 Mixpipes

With Mixpipe 1 as a baseline each mixpipe were made in an effort to increase power induced in the mixer, rather than the mixpipe, and all resulted in various degrees of improvement. The first, Mixpipe 1, is just a regular pipe which for all intents and purposes is what's used today. As can clearly be seen in the results of Mixer 1 Mixpipe 1 this is not an efficient solution with almost all power induced in the wall and barely anything in the mixer as shown in

figure 20. The heat transferred to the exhaust is therefore minimal and not a suitable solution. The first improvement, Mixpipe 2, was based on the idea of removing a strip of the wall exposing part of the mixer wall directly to the windings, allowing induction to occur directly in the mixer wall. This resulted in some slight improvements, as seen in figure 23, but nowhere near what's needed and was therefore also discarded from use with the other mixers. Mixpipe 3 was based on the idea of restricting the possibility for current to flow in the pipe wall, while also letting the magnetic field reach the mixer, by cutting a hole in the wall at each mixer blade. As seen in the results of Mixer 1 Mixpipe 3 this resulted in a rather large efficiency gain, improving the power induced in the mixer almost tenfold which can be seen in figure 27. The drawbacks were still that a lot of power was induced in the mixpipe rather than the mixer but even more alarmingly was that the edges of the slits became warm spots because of current trying to move from one side of the slit to another had to pass by the edges, resulting in an increased current concentration which led to temperatures nearing the steels melting point. The next improvement, Mixpipe 4, increased the number of slits five-fold which significantly reduced the power induced in the walls by making it even harder for the current to flow in the pipe. This was the first mixpipe where more power was induced in the in the mixer than the mixpipe, seen in figure 30, which was a major milestone and the first mixpipe to show some promise of being a plausible solution to the problem. It was therefore decided that this mixpipe was to be simulated using each mixer design. Lastly, the fourth improvement, Mixpipe 5, was made with a different approach. Instead of having a wall which the magnetic field has to pass through with windings tightly wound on the outside, instead the windings could make up the wall. This approach present several key advantages. Firstly, it has the potential to have very low to no loss in the mixpipe depending on the distance of the gap between windings and the edges of the mixpipe for the magnetic field to flow through, which means nearly all induction would occur in the mixer where it's wanted. Judging by the results of Mixpipe 5 it's clear that the distance between winding and mixpipe of about 9 mm used in the simulations wasn't enough distance for the magnetic field to pass through since the pipe edges reached a temperature of nearly 500° C in four seconds and an induced power of over 4000 W. The second advantage of this design is that the windings would be closer to the mixer, increasing the induced power substantially since the strength of the magnetic field decreases exponentially with distance. From a performance viewpoint Mixpipe 5 is the superior alternative, but it might also present a challenge to construct and implement in a truck.

7.3 Validation

Comparing the validation build to the simulations there are some points worth noting. The validation build consistently achieved higher temperature than the simulations, this can be seen in figure 49 compared to figures 88 and 90 as well as figure 50 compared to figures 89 and 91. Some explanations for the higher temperature in the validation are approximations and boundary conditions for the simulations. A boundary condition was applied to the surface of the mixer where it approximated all the induced currents to the surface of the mixer. The stainless steel the mixer was made of had a specified permeability of 2000 which only is true for certain conditions. The permeability simulated was modeled to have a curie temperature but magnetic saturation was not included in the model. In the model the currents were modeled to run through a line around the mixer and mixpipe where the currents in the build most likely were more spread out in the copper tubing. The exact placement of the components in the build may also have some variations compared to the simulations. Both the mixer and mixpipe were designed to be close to the same size as the models but they both received some modifications in order to fit in a good way.

One thing that the validation build and the simulations have in common is the way that the mixer is heated. Comparing figure 49 with figures 88 and 90 it is notable that at 4 seconds the validation build and simulation model have a similar looking heating where the sharp corner at the bottom of the mixer blade has received the most notable heating. Apart from that point the blades has also started to heat up in both validation build and model. Looking at figure 50 and comparing with figure 91 it can be seen that the sharp corner still is the hottest and that the heat has transferred further out in the blades. It can also be seen a belt around the mixer wall, at about the height of the sharp corner, stands out from the rest of the mixer in terms of heating. These similarities in the heating pattern of the validation build and simulation suggest that the heating in the simulation correlates well with reality.

7.4 Conclusions

There certainly is a potential to heat the exhaust gases at cold starts well enough for the system to handle the NO_x but there are certain changes needing to be made in order for it to work. Changes we made in order to induce heat in the mixer blades are:

- slits in the mixpipe in order for the magnetic field to reach the mixer

- Material change in the mixer from austenitic stainless steel to ferritic stainless steel to increase the heating of the mixer
- Upwards angling of the mixer blades to avoid the shielding of the mixer wall

With these changes power can be induced in the blades of the mixer but there are still problems that needs to be handled. In the mixers based on the existing design there remains the sharp corner at the bottom of the mixer blade, for mixpipes 3 and 4 there are sharp corners at the end of the slits. These sharp corners needs to be addressed in some way as currents forced past these corners heat them up much faster than the rest of the design. Heating up the mixer wall within seconds is certainly possible and with a more optimized design so should be the case for the mixer blades as well.

8 Improvements and further work

Since our models and modifications are built with the purpose of inducing power in the mixer blades there are things needing to be worked on for this to be ready to use. The sharp corners both in the mixer and mixpipe require modification of some sort. Both removing windings and rounding off the corners are suggested solutions that should be looked more closely at, but perhaps most effective would be to redesign a mixer without this issue. Since our models are made with another mixer material and in some cases with holes in the mixpipe this would also need to be looked at to fill the holes in the mixpipe and evaluate if the mixer material would work in the exhaust system. One of the most important points for further work is to run the mixer and mixpipe combinations through a computational fluid dynamics simulation. Our changes of the mixer and mixpipe did not take into consideration the effect it would have on the exhaust gas flow and since that is currently the mixers primary function it needs to handle that part in a satisfactory way.

9 Bibliography

[1] European Environment Agency. *EU: Heavy-Duty Truck and Bus Engines*. Apr. 21, 2017. URL: https://www.eea.europa.eu/data-and-maps/indicators/eea-32-nitrogen-oxides-nox-emissions-1.

[2] Dieselnet. *Nitrogen oxides (NO_x) emissions*. Apr. 26, 2017. URL: https://www.dieselnet.com/standards/eu/hd.php.

[3] Felix Birkhold et al. *Analysis of the injection of urea-water-solution for automotive SCR DeNOx-systems: modeling of two-phase flow and spray/wall-interaction*. Tech. rep. SAE Technical Paper, 2006.

[4] Karin Jonasson. "Analysing hybrid drive system topologies." In: (2002).

[5] David K. Cheng. *Field and Wave Electromagnetics*. Pearson Education, 2013. ISBN: 9781292026565.

[6] Jim Breithaupt. *Physics, Third edition*. Palgrave Macmillian, 2010. ISBN: 9780230231924.

[7] E.J. Davies. *Conduction and induction heating*. Peter Peregrinus Ltd., London, United Kingdom, 1990. ISBN: 0863411746.

[8] Frogner, K; Andersson, M; Cedell, T; Siesing, L; Jeppson, P; Ståhl, J-E. "Industrial heating using energy efficient induction technology." In: *44th CIRP Conference on Manufacturing Systems, 2011 - Madison, Wisconsin, United States* (2011).

[9] www.electronics-tutorials.ws. *Magnetic Hysteresis loop*. Apr. 3, 2017. URL: http://www.electronics-tutorials.ws/electromagnetism/magnetic-hysteresis.html.